

---

Masters Theses

Student Theses and Dissertations

---

1973

## A study of the ability of surface active materials to increase the evaporation rates of small, freely falling water drops

David Alan Sierawski

Follow this and additional works at: [https://scholarsmine.mst.edu/masters\\_theses](https://scholarsmine.mst.edu/masters_theses)

 Part of the [Chemistry Commons](#)

Department:

---

### Recommended Citation

Sierawski, David Alan, "A study of the ability of surface active materials to increase the evaporation rates of small, freely falling water drops" (1973). *Masters Theses*. 3362.  
[https://scholarsmine.mst.edu/masters\\_theses/3362](https://scholarsmine.mst.edu/masters_theses/3362)

This thesis is brought to you by Scholars' Mine, a service of the Missouri S&T Library and Learning Resources. This work is protected by U. S. Copyright Law. Unauthorized use including reproduction for redistribution requires the permission of the copyright holder. For more information, please contact [scholarsmine@mst.edu](mailto:scholarsmine@mst.edu).

A STUDY OF THE ABILITY OF SURFACE ACTIVE  
MATERIALS TO INCREASE THE EVAPORATION RATES  
OF SMALL, FREELY FALLING WATER DROPS

BY

DAVID ALAN SIERAWSKI, 1948-

A THESIS

Presented to the Faculty of the Graduate School of the

UNIVERSITY OF MISSOURI-ROLLA

In Partial Fulfillment of the Requirements for the Degree

MASTER OF SCIENCE IN CHEMISTRY

1973

T2920  
81 pages  
c.1

Approved by

*J. F. Stampfer* (advisor) *John C. Carstens*  
*D. Vincent* *Loach*

## ABSTRACT

The evaporation rate at 30°C of water droplets partially covered by surface active materials (SAM) were determined. While two of the SAM were studied at a single dew point depression ( $\Delta T_{DP}$ ), seven others were examined over a range of  $\Delta T_{DP}$  values. It was found, by comparison with pure water drops under identical conditions, that SAM increases the evaporation rate as compared to the rate of an uncontaminated drop. The lack of effect of the hydrophobic chain length and the possible effect of the hydrophilic group on this phenomenon are discussed. The explanation proposed is that at 30°C thermal agitation of the hydrophobic chain causes a breakdown of the water structure and imparts extra energy to the molecules in the vicinity of the SAM. This corresponds to an elevation of the local temperature near the SAM and causes the overall evaporation rate of the drop to increase.

## ACKNOWLEDGEMENTS

The author is indebted to Dr. J. F. Stampfer, Jr. for his advice throughout the course of this work. Thanks are also extended to Drs. J. C. Carstens and D. V. Roach for their helpful criticism of this manuscript. The assistance of Mrs. Kathryn Berkbighler in the data analysis is also acknowledged.

This work has been supported by the National Science Foundation Grant NSF GA-1509.



## TABLE OF CONTENTS

	Page
ABSTRACT . . . . .	ii
ACKNOWLEDGEMENTS . . . . .	iii
LIST OF FIGURES . . . . .	vi
LIST OF TABLES . . . . .	vii
I. INTRODUCTION . . . . .	1
II. BACKGROUND . . . . .	2
A. Atmospheric Surface Active Materials . . . . .	2
1. Hydrocarbons in the atmosphere . . . . .	2
2. SAM in the atmosphere . . . . .	3
B. Evaporation of Uncontaminated Drops . . . . .	4
C. Evaporation of Contaminated Drops . . . . .	5
1. Retardation of evaporation by monolayers . . . . .	5
2. Enhanced evaporation by SAM . . . . .	8
a. Enhanced evaporation by SAM under nonsteady state conditions . . . . .	8
b. Enhanced evaporation by SAM monolayers . . . . .	9
c. Enhanced evaporation at low concentrations of SAM . . . . .	12
D. Effect of Foreign Materials on Water Structure . . . . .	14
III. APPARATUS . . . . .	18
A. Drop Generator . . . . .	18
B. Drift Tube . . . . .	20
C. Humidifying System . . . . .	21
D. Water Baths and Temperature Sensors . . . . .	23

	Page
E. Nuclei Generating Systems . . . . .	23
F. Camera System . . . . .	27
IV. EXPERIMENTAL PROCEDURE . . . . .	29
V. RESULTS . . . . .	32
VI. EXPERIMENTAL ERROR . . . . .	50
VII. DISCUSSION OF RESULTS AND CONCLUSIONS . . . . .	55
REFERENCES . . . . .	67
VITA . . . . .	72
APPENDIX - LIST OF SYMBOLS . . . . .	73

## LIST OF FIGURES

	Page
Figure 1. Drop generator and drift tube . . . . .	19
Figure 2. Overall block diagram of humidification system . . . . .	22
Figure 3. Nuclei generating system (trough method) . . . . .	25
Figure 4. Nuclei generating system (atomizer-impactor method) . . . . .	26
Figure 5. Evaporation rates of uncontaminated water drops at 30°C . . . . .	38
Figure 6. Evaporation rates of dodecanol contaminated water drops at 30°C . . . . .	39
Figure 7. Evaporation rates of Igepal CO-430 contaminated water drops at 30°C . . . . .	40
Figure 8. Evaporation rates of Igepal CO-730 contaminated water drops at 30°C . . . . .	41
Figure 9. Evaporation rates of hexadecane contaminated water drops at 30°C . . . . .	42
Figure 10. Evaporation rates of decanoic acid contaminated water drops at 30°C . . . . .	43
Figure 11. Evaporation rates of ethyl myristate contaminated water drops at 30°C . . . . .	44
Figure 12. Evaporation rates of ethyl caprate contaminated water drops at 30°C . . . . .	45

## LIST OF TABLES

	Page
Table 1. Data obtained for an evaporating droplet with magnification factor = 5.8 . . .	33
Table 2. Physical constants . . . . .	35
Table 3. Comparison of data for uncontaminated drops at 30°C . . . . .	37
Table 4. Linear least squares coefficients . . . . .	46
Table 5. Quadratic least squares coefficients . . . . .	47
Table 6. Comparison of data for dodecanol contaminated drops at 30°C . . . . .	48
Table 7. Results of compounds studied at a single dew point depression . . . . .	48
Table 8. Enhanced evaporation rates at $T_2 = 35.0^\circ\text{C}$ . . . . .	49
Table 9. Frequency of occurrence of the sign of $\gamma_Q$ as a function of the percentage change of the radius . . . . .	58

## I. INTRODUCTION

With an increase in human population and activities, a new emphasis has been placed on understanding the effects of the products of man's activities on the environment. Scientists have become increasingly aware of the need to comprehend present atmospheric processes and how they may be altered. Chemical compounds, released into the atmosphere, provide a possible source of difference in the behavior of droplets of atmospheric origin and pure water droplets.

To increase our knowledge of one possible effect of chemicals on the atmosphere, a study has been undertaken to determine the effect of surface-active materials (SAM) on the evaporation rate of water droplets of about  $3\text{-}10\mu\text{m}$  radius. Droplets of this size and smaller are formed within clouds and are the predecessors of raindrops. They may also be present in regions of high relative humidity. Any SAM present in the atmosphere may be incorporated into these water droplets. Therefore, any effects of SAM on the stability or instability of the drops is of special interest to atmospheric studies.

Although the effects of a monolayer coverage of SAM on water droplets have been studied in the past, there are very few data on partial coverage. Our studies are intended to fill the gap in this area of knowledge.

## II. BACKGROUND

### A. Atmospheric Surface Active Materials

To apply the data obtained in this study to atmospheric processes, it should be shown that there are surface active materials (SAM) in the atmosphere. SAM, chemical compounds which have an energetic tendency to congregate at an interface, have been verified to exist in rain samples. Further details are presented below. Also, for these data to apply, the drops must possess only partial coverages.

#### 1. Hydrocarbons in the atmosphere

There have been considerable data collected on the concentration of hydrocarbons in the atmosphere. The work of Altshuller (1) provides some data on the concentrations of medium weight hydrocarbons, e.g. 1-pentene and 2-methyl 2-butene, in a polluted atmosphere. Another report from the Stanford Research Institute (2) tabulates many sets of data on hydrocarbons in the atmosphere, estimating that the total hydrocarbon emission by human activity is 88 million tons/year. In the same report (2) is a tabulation of the data of F. W. Went, who estimates that the total emission of terpene-like materials into the atmosphere by vegetation is 170 million tons/year, a number which is comparable to the 88 million tons/year emitted by man.

These data do not prove that SAM are present in the atmosphere, but they do provide an idea of the large amounts

of complicated molecules that can be transported into and exist in air.

## 2. SAM in the atmosphere

Organic material at the sea surface is one important source of SAM in the atmosphere. Blanchard (3) has collected droplets of surf spray on fine platinum wires. He found evidence of SAM on all the wires exposed to the sea spray. In a similar study Barger and Garrett (4) collected offshore samples of marine air on paraffin-coated trays and also with filters. Both methods indicated the presence of SAM. Fatty acids from  $C_{14}$ - $C_{18}$  were found to be present in the same relative proportions as in sea surface samples.

Studies have been carried out at the University of Missouri-Rolla (5) on the SAM content of precipitation. The amount of SAM in samples of precipitation was measured with a modified Langmuir film balance. These all showed evidence of SAM with amounts varying from 0.5 to greater than  $10 \text{ cm}^2/\text{ml}$  of precipitation at 5 dynes film pressure. Assuming that these materials are present in the atmosphere as particulate matter which then act as condensation nuclei, or are scavenged in the cloud by the cloud droplets, it is reasonable to expect at least partial surface coverage of many of the cloud drops. For example, if we assume that the drops collected in  $1 \text{ cm}^3$  of precipitation originally were 1.0 mm in radius, their total surface area would have been about  $30 \text{ cm}^2$ . Since only about  $10 \text{ cm}^2$  of SAM were found,

partial coverage of the drops with SAM is considered likely.

#### B. Evaporation of Uncontaminated Drops

In 1877 Maxwell proposed a diffusion theory for droplet evaporation (see Fuchs (6)). Maxwell's model for stationary state evaporation assumed that the evaporation rate depended only on the rate of diffusion of evaporating molecules through the surrounding gaseous media. In addition, the drop was spherical and stationary with respect to the surrounding gas. It was also assumed that the vapor concentration at the drop surface was the saturation value at the temperature of the drop and that the evaporation was a steady state process. Maxwell's equation can be written as\*

$$-\frac{d(a^2)}{dt} = \frac{2D}{\rho_1} (\rho_s - \rho_\infty) = I_M \quad (1)$$

Fuchs (7) solved the drop evaporation problem using both mass and heat diffusion. The additional assumptions of this model were that only conductive heat transfer was important and that the coefficient of thermal conductivity was constant in the surrounding gas. Fuchs' modification of Maxwell's equation can be written (8) as

$$-\frac{d(a^2)}{dt} = \frac{2D}{\rho_1} \frac{\Gamma b}{\Gamma + b} (T_\infty - T_{DP}) = \beta_M (\Delta T_{DP}) \quad (2)$$

\*See Appendix for the definitions of the symbols used here and elsewhere in this report.



Further, Fuchs (6) postulated, in analogy with the sharp gradient of temperature near a heated or cooled surface, that the vapor concentration would exhibit a sharp gradient, or jump over a distance on the order of a mean free path near the drop surface. This result can be written as

$$I_F = - \frac{d(a^2)}{dt} = \frac{I_M}{\frac{D}{av\alpha} + \frac{a}{a + \Delta}} \quad (3)$$

Other corrections have been proposed for small, evaporating water droplets and further information can be found in a previous paper (8) and thesis (9). These corrections appear to be negligible for our studies.

Duguid (8) and Hughes (10) have collected information on the rate of evaporation of uncontaminated water drops at three temperatures: 25, 30 and 35°C. Duguid has found that the evaporation rates obtained experimentally agree best with the simple diffusion theory.

### C. Evaporation of Contaminated Drops

#### 1. Retardation of evaporation by monolayers

Derjaguin et al. (11) have studied the evaporation rate of 300µm radius drops. They found that drops previously exposed to a saturated vapor of hexadecanol exhibited a slower evaporation rate, than those of uncontaminated drops. The contaminated drops were supported on glass filaments in

a controlled environment containing hexadecanol vapors. When placed in a second chamber, where they evaporated, the drops exhibited two steps in the evaporation process. Initially, the drops evaporated rapidly, at the same rate as pure drops. However, after a time, which was a function of the length of exposure to the hexadecanol vapors, the evaporation rate showed an approximate tenfold decrease. This was attributed to the formation of a monolayer.

Snead and Zung (12), using a Millikan Oil Drop Apparatus, have collected data on the evaporation rates of 1-5 $\mu$ m radius water droplets treated with n-decanol. They also observed two steps in the evaporation which was attributed to the formation of a monolayer and a consequent decrease of about a thousandfold in the evaporation rate.

Working with water mists, Eisner, Quince and Slack (13) found that small quantities of fatty alcohols, when added to water to achieve initial concentrations of 0.05-0.2%, would markedly increase the lifetime of a mist. These mists, containing 2-90 $\mu$ m radius droplets, were generated and allowed to fall in a vertical tube. Size distributions were determined by taking samples at the top and bottom of the tube. Calculated lifetimes of the droplets increased from 80 to 500 times, as the initial radius varied from 40 to 5 $\mu$ m. The prolonged lifetimes were attributed to a decrease in the evaporation coefficient,  $\alpha$ , due to the presence of the fatty alcohol monolayers.

Kocmond, Garrett and Mack (14) have also studied the

effects of long chain alcohols on water mists. In their work fog droplets in a  $600\text{ m}^3$  chamber were coated with hexadecanol, which was introduced in controlled amounts in the vapor phase and allowed to condense on or be scavenged by the pre-existing water droplets, until it was reasonably certain a monolayer had formed. The changes in visibility with time were compared to results with uncoated drops in an identical chamber. The chamber containing SAM-coated droplets showed markedly reduced visibilities, indicating stabilization of the drops by the hexadecanol.

In another study Garrett (15) attempted to obtain data closer to actual atmospheric conditions. It is known that SAM exist at the sea-water interface and that they can be transported into the atmosphere by bursting bubbles and sea spray (3). However, few of these are likely to be of the linear, tightly-packed variety, i.e. possessing a hydrophilic group attached to an n-alkane chain. Garrett studied a number of SAM and found that when molecules can no longer pack tightly in a monolayer (e.g. by being unsaturated or possessing any functional group which increases the surface area/molecule over that of the linear alkyl chain), the monolayer's ability to retard evaporation was greatly reduced. These SAM produced little or no reduction in the evaporation rate from that of pure water. Ineffectiveness in reducing the evaporation rate has also been observed in plane surfaces (16) when impurities, such as benzene, remain in a monolayer which normally exhibits evaporation

retardation.

## 2. Enhanced evaporation by SAM

The data in the literature which indicate evaporation rate enhancement by SAM have been collected primarily in three types of circumstances 1) nonsteady state conditions 2) monolayer coverages 3) low concentrations of SAM. These are discussed separately below.

### a. Enhanced evaporation by SAM under nonsteady state conditions

Tovbin and Savinova (17) studied the evaporation rates from SAM-water jets immediately (0.001-0.02 sec) upon emergence from a nozzle. At air contact times less than 0.003 sec, they found the evaporation rates of the SAM-water jets to be significantly higher than that of a pure water jet. The explanation for this phenomena was given in terms of an "interphase, self-adsorption layer". During the initial period of exposure to air, the water molecules are involved in forming this self-adsorption layer and are not carried off by the gaseous flow around the drop. From these data it appears that this adsorption for a pure surface takes about 0.003 sec. Afterwards, the normal evaporation rate is observed. When SAM is present on the surface, the number of water molecules required to form the self-adsorption layer is less. Therefore, the normal evaporation rate is restored earlier than 0.003 sec. This makes the

average rate at times  $< 0.003$  sec appear larger in the presence of SAM.

James and Berry (18) studied evaporation rates of water solutions by a gravimetric method. They found that ovalbumin and hemoglobin solutions exhibited higher evaporation rates than pure water. Knowing that these proteins possessed a large sphere of hydration, James and Berry proposed that the proteins were being adsorbed at the surface where disruption of the sphere of hydration occurred. Thus, the surface region possessed excess water molecules, causing an increased evaporation rate. James and Berry also mentioned that other studies (19) with monolayers of proteins did not show an increase in the evaporation rate.

Bull (20), in studying the surface denaturation of protein-water solutions, noticed that evaporation from a rotating drum was much greater for these solutions than for pure water. He did not observe this same effect on a quiescent surface.

b. Enhanced evaporation by SAM monolayers

Derjaguin (21) has stated that a monolayer, depending on its nature, may accelerate as well as retard the evaporation rate. This was shown theoretically with both quasistationary and nonstationary models. In the quasistationary case, the evaporation rate for a pure liquid drop is given by

$$-\frac{dm}{dt} = \frac{m_1 (C_o - C_\infty) 4\pi a^2}{\frac{1}{D} \frac{a^2}{a + \Delta} + \frac{1}{\alpha_o \bar{v}/4}} \quad (4)$$

while for the same drop covered by a film

$$-\frac{dm}{dt} = \frac{m_1 (C_o - C_\infty) 4\pi a^2}{\frac{1}{D} \frac{a^2}{a + \Delta} + \frac{C_o}{C_p} \frac{\delta}{D_1} + \frac{1}{\alpha_o \bar{v}/4}} \quad (5)$$

Thus, differences in the evaporation rates will be reflected by differences in the two terms

$$\frac{1}{\alpha_o \bar{v}/4} \text{ and } \frac{C_o}{C_p D_1} \frac{\delta}{D} + \frac{1}{\alpha_o \bar{v}/4} \quad (6)$$

When the latter is smaller, the evaporation rate of the film-covered drop will be higher than that of the pure drop. In the nonstationary case, the rate of evaporation is given as a function of time. The rate at  $t = 0$  for a flat surface has been solved and has the form

$$r|_{t=0} = r_o \left( 1 + \frac{\alpha \bar{v}}{4} \frac{\ell - \Delta}{D} \right) \quad (7)$$

Thus, depending on the values of  $\alpha$  and  $D$ , the evaporation rate can be greater initially for a film-covered drop than for a pure drop.

Zung (22) has concluded, theoretically, that an increase in the evaporation coefficient due to the presence of SAM could increase the evaporation rate, due either to the nature of the SAM or curvature effects on the molecular arrangements of the monolayer. His result for the evaporation rate of a film-covered droplet was

$$I_Z = - \frac{dm}{dt} = \frac{4\pi a D m_2 (C_o - C_\infty)}{\frac{D}{\alpha \bar{v}/4} \frac{a}{(a + \delta)^2} + \frac{a}{(a + \delta + \Delta)} + \frac{D}{D_1} \frac{C_o}{C_p} \frac{\delta}{a + \delta}} \quad (8)$$

The result for a pure droplet was identical to eq. 4.

O'Grady (23) has carried out a study of the evaporation coefficients of water in the presence of dissolved salts and SAM. He found that the evaporation coefficient increased from 0.12 for a 3.5 wt. % NaCl-water solution to 0.26 for the same solution in the presence of an Igepal compound, CO-730 (Igepal is a product and tradename of the GAF Corporation for nonylphenoxy-ethyleneoxyethanol compounds). O'Grady simply concluded that the effect on the evaporation coefficient was definitely due to the presence of the Igepal compound. O'Grady also studied the effects of hexadecanol and oleic acid films on distilled, deionized water. These films possessed evaporation coefficients of 0.006 and 0.08 respectively. These values are lower than the evaporation coefficient found for uncontaminated water by O'Grady ( $\approx 0.2$ ), and hexadecanol and oleic acid should therefore lower the

evaporation rate from that of pure water. Igepal CO-730, however, should elevate the evaporation rate of a 3.5 wt. % NaCl solution. The three SAM were present in sufficient concentrations to form monolayers.

The use of Igepal CO-730 by O'Grady was initiated because of a patent issued to Beredjick (24). In this patent Beredjick states that Igepals, both soluble and insoluble, increase the evaporation rate of water by about 20%.

c. Enhanced evaporation at low concentrations of SAM

Leonov and Prokhorov (25) have studied the evaporation of 3-4 $\mu$ m radius drops suspended on filaments. In general, they concluded that SAM inhibits evaporation. However, for two compounds examined, quartolite and hexyl alcohol, the evaporation rates were higher than that of pure water when the concentrations of SAM were less than 0.01%. They attempted no explanation of this phenomenon but stated that the increase in the rate was beyond experimental error limits.

In work inspired by his previous studies on tungsten filaments with cesium impurities, Kingdon (26) studied the evaporation rate of a water surface in the presence of adsorbed foreign gases. He employed various gases, including hydrocarbons, to provide imperfection sites on the water surface. Using a mass spectrometer as a detector, Kingdon found evidence for evaporation proceeding by spurts



in the presence of most of these gases. His explanation was that, when a foreign molecule was adsorbed on the surface, some of the neighboring water molecules would form weaker hydrogen bonds with the nonpolar adsorbate than with other water molecules. This then led to a spurt of water from the region around the adsorbed molecule. The spurt would be stopped by the local cooling accompanying the increased evaporation.

Hughes (10) has studied the effect of dodecanol and hexadecanol on the evaporation rate of 3-10 $\mu$ m radius water drops. The drops were generated in a thermal diffusion cloud chamber, either on room air nuclei, to obtain uncontaminated drops, or on nuclei of SAM, for contaminated droplets. In the case of uncontaminated drops at 30°C, Hughes obtained an evaporation rate of

$$-\frac{d(a^2)}{dt} = 19.6 \Delta T_{DP} + 0.1 \quad (9)$$

which agrees well with the previous data of Duguid (9)

$$-\frac{d(a^2)}{dt} = 19.1 \Delta T_{DP} + 0.2 \quad (10)$$

This work provided a baseline for the effects of SAM on the evaporation rate. For drops at 30°C contaminated with dodecanol, Hughes obtained

$$-\frac{d(a^2)}{dt} = 17.8 \Delta T_{DP} + 1.6 \quad (11)$$

while for hexadecanol contaminated drops the result was

$$-\frac{d(a^2)}{dt} = 18.0 \Delta T_{DP} + 1.8 . \quad (12)$$

As the surface coverage of the SAM contaminated drops was estimated to be about 10% of the total surface area, this difference, indicating an increase in the evaporation rate, was attributed to the presence of SAM at concentrations yielding partial surface coverages.

#### D. Effect of Foreign Materials on Water Structure

Drost-Hansen (27), in studies of water structure, has noted that there is structural enhancement of water near a monolayer of SAM, similar to that near a solid surface. However, he also proposes that there is more than one form for this structure, and that near 30°C there is a conversion from one form to the other in the layers near the monolayer. This hypothesis is based on many reported instances of unusual water properties between 29-32°C. One of these anomalies indicates an abnormally high value of the surface entropy at 30°C. To explain this, Drost-Hansen proposed that the enhanced structuring of water occurs not only near a monolayer, but also in the region of SAM monomers and aggregates. Since the anomalies at about 30°C are related to a transition between two different structures of water near SAM, this transition could produce an unusually high number of monomeric water molecules and an unusually high

surface entropy. Drost-Hansen also predicted that these excess water monomers should produce a higher evaporation rate near 30°C.

It has long been known that simple ionic solutes can change the structure of bulk water. These effects have been noted in studies of heat capacity, dielectric relaxation, thermal conductivity, temperature of maximum density, ion mobility, entropy of dilution and viscosity. There has also been increasing attention paid to the effects of larger organic ions, such as tetraalkyl ammonium salts, and to soluble nonionic organic substances, such as t-butyl alcohol. Rather than review this literature in detail, we refer only to a number of general works on the subject (28,29,30). In the discussion section below, specific references will be made to pertinent papers.

It is generally agreed that water, due to the presence of hydrogen bonds, has greater structure than is present in liquids which do not have the capability of forming these or similar bonds. It is this structure which is the cause of many of the abnormal properties of liquid water, e.g. its high boiling point. The presence of a solute in otherwise pure water will undoubtedly have an effect on the hydrogen bonding, either increasing or decreasing the amount of structure. It is known (31) that certain electrolytes will enhance water structure, e.g. NaCl, while others have the opposite effects, e.g. KCl. While the materials used in this study are not considered electrolytes and reside in the

surface rather than the bulk, they may also enhance or disrupt the structure, and in this way affect the evaporation.

Jolicouer (32) has studied the differential infrared absorption spectra of water between 0.8 and 1.2  $\mu$ m. When  $\text{Bu}_4\text{NBr}$  was added to the water, a spectrum was produced indicating the same effect on the hydrogen bonding as a decrease in temperature. This compound was classified as a structure maker. However, for  $\text{NaB}(\text{C}_6\text{H}_5)_4$  the opposite effect was observed. The differential spectrum of this compound showed an effect on the hydrogen bonding analogous to an increase in the temperature and  $\text{NaB}(\text{C}_6\text{H}_5)_4$  was classified as a structure breaker.

Davies, Ormondroyd and Symons (33) have examined the proton nuclear magnetic resonance shifts of water over a temperature range of 0-80°C with tetraalkylammonium ions present. At 30°C the proton NMR shifts of solutions of the ethyl, propyl and butyl compounds pass from negative to positive, corresponding to a transition from a more ordered structure (below 30°C) to less ordered structure (above 30°C) than that present in pure water. The tetramethyl ammonium bromide and octyl trimethyl ammonium bromide solutions were exceptions to this transition, the former remaining more ordered throughout the temperature range studied, and the latter possessing less order or hydrogen bonding than pure water. They conclude that at elevated temperatures disorganization, or less hydrogen bonding, is

enhanced by long chain alkyl groups.

Wen (34) has discussed NMR studies with solutions of tetraalkyl ammonium bromide and nitrate salts at 25°C. A positive shift relative to pure water was observed, i.e. the same effect as an increase in temperature. Also, the shift increases to greater positive values as the cation size, or alkyl chain length increases.

### III. APPARATUS

The essential parts of the apparatus are described below. For further details two previous papers (8,10) may be helpful since, except for the nuclei generating system, the equipment is nearly identical.

Droplets of 3-10 $\mu$ m radius were formed in a thermal diffusion cloud chamber and allowed to fall freely through a thermostated drift tube. The positions of the drops in the drift tube were determined at 0.5 sec intervals by photographing them. Subsequent determination of the terminal velocities allowed the radii of the drops to be calculated. The parameter  $-d(a^2)/dt$  was taken as the evaporation rate of the droplets. The humidity in the drift tube was controlled by passing air, saturated with water vapor at temperature  $T_1$ , through the drift tube immediately prior to the run. The drift tube itself was maintained at a higher temperature,  $T_2$ . The difference,  $T_2 - T_1$ , is called the dew point depression,  $\Delta T_{DP}$ . By changing  $T_1$ , the water vapor content of the drift tube could be varied to obtain the evaporation rates at different dew point depressions.

#### A. Drop Generator

The thermal diffusion cloud chamber (see Fig. 1) was constructed with two circular plates (15 cm dia.) separated by a 2.5 cm high by 14 cm diameter lucite tube. This

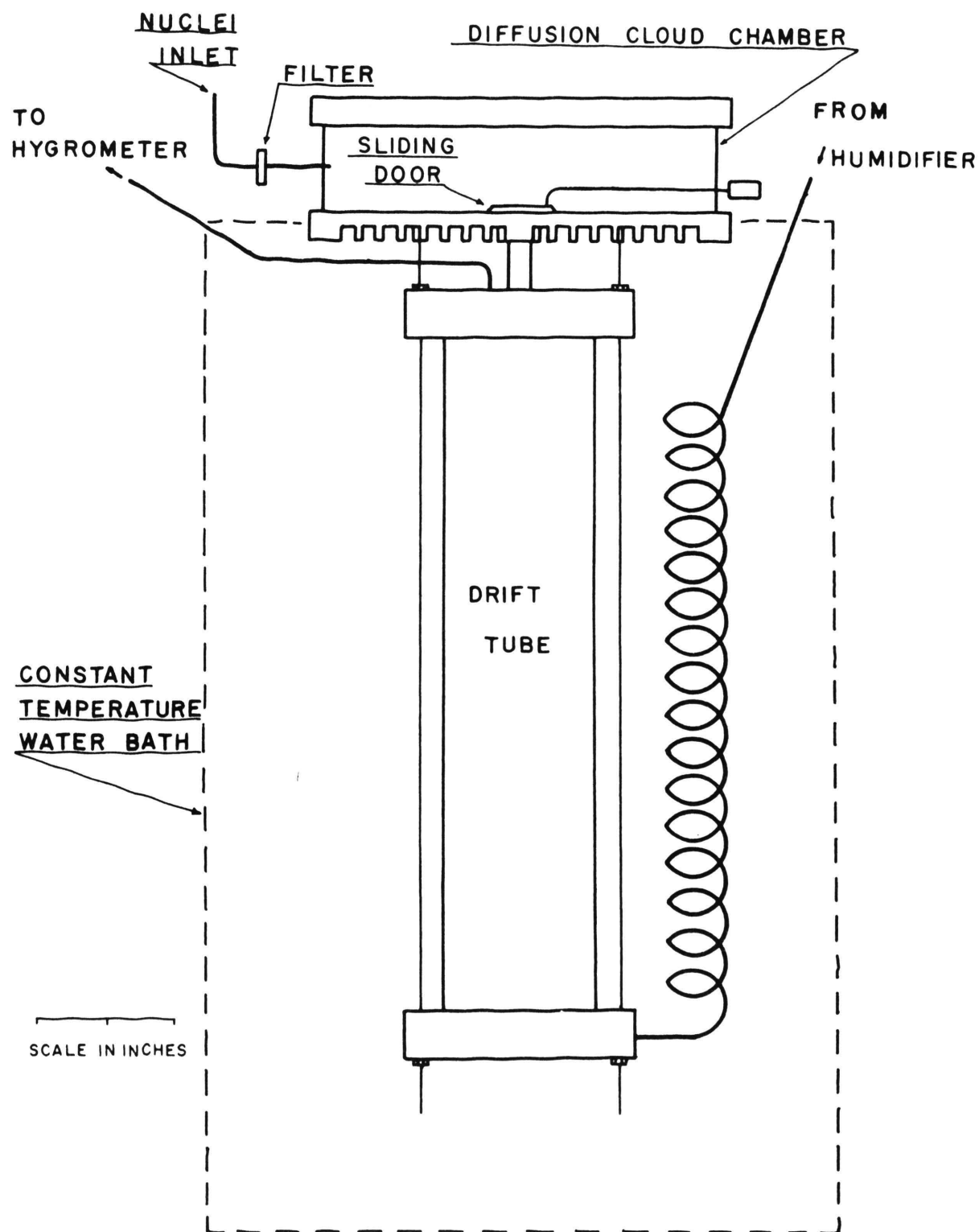


Fig. 1. Drop generator and drift tube (8)

lucite window was maintained free of condensation by nichrome heating wires so that the drops in the chamber could be observed. Within the top plate were additional nichrome heating wires, arranged in epoxy-filled concentric grooves. A sintered, porous plate ( $5\mu\text{m}$  pore size) covered a water reservoir on the underside of the upper plate. The bottom plate had a 0.6 cm hole in the center through which the drops could fall. A sliding door, controlled by a rod through the side wall, covered this hole. A 2.5 cm long copper tube was threaded into this hole to collimate the drops as they fell into the drift tube. The area around the hole was slightly elevated so that water, collecting on the bottom plate, could not easily fall into the drift tube.

#### B. Drift Tube

The side walls of the drift tube (see Fig. 1) were constructed of 25 cm x 5 cm sheets of double-thick plate glass. These were sealed with Dow Corning Silastic 732 RTV to form a 5 cm x 5 cm square tube. The top and bottom were sealed with two 2 cm thick pieces of teflon and rubber gaskets. The bottom piece was drilled to permit entry of humidified air. In the top piece were two threaded holes; one allowed the humidified air to be exhausted, while the other was used to attach the copper tube connection from the cloud chamber. Both the drift tube and bottom plate of the cloud chamber were immersed in a constant temperature bath, held at temperature  $T_2$ .



### C. Humidifying System

The humidifying system consisted of two units, the prehumidifier and humidifier (refer to Fig. 2). The prehumidifier was a 1 liter round bottom flask partially filled with water and heated to about 40°C with a hot plate. Filtered room air was pumped, at about 2 liters/minute, through this flask.

The prehumidified air then passed through the humidifier, which was a 30 cm x 30 cm x 5 cm lucite box, filled to within 1 cm of the top. The inside of the box was partitioned so that the air flow was constrained to a 7.5 m path over the water surface. The entire box was submerged in a constant temperature bath held at temperature  $T_1$ . The air emerging from the humidifier was assumed to be saturated with water vapor at the temperature  $T_1$ . The humidified air then entered the drift tube after passing through a 3.75 m, 1/4 in I.D., copper coil, immersed in the same constant temperature bath as the drift tube. Thus, when this air entered the drift tube, the temperature was  $T_2$  and the water vapor content was fixed corresponding to a dew point temperature of  $T_1$ . Therefore, the dew point depression was simply the difference between the temperature of the drift tube,  $T_2$ , and the temperature of the humidifier,  $T_1$ .

The various parts of the humidifying system were connected by 1/4 in I.D. copper tubing. Wherever the copper tubing was exposed to room air it was heated to prevent condensation of the water vapor.

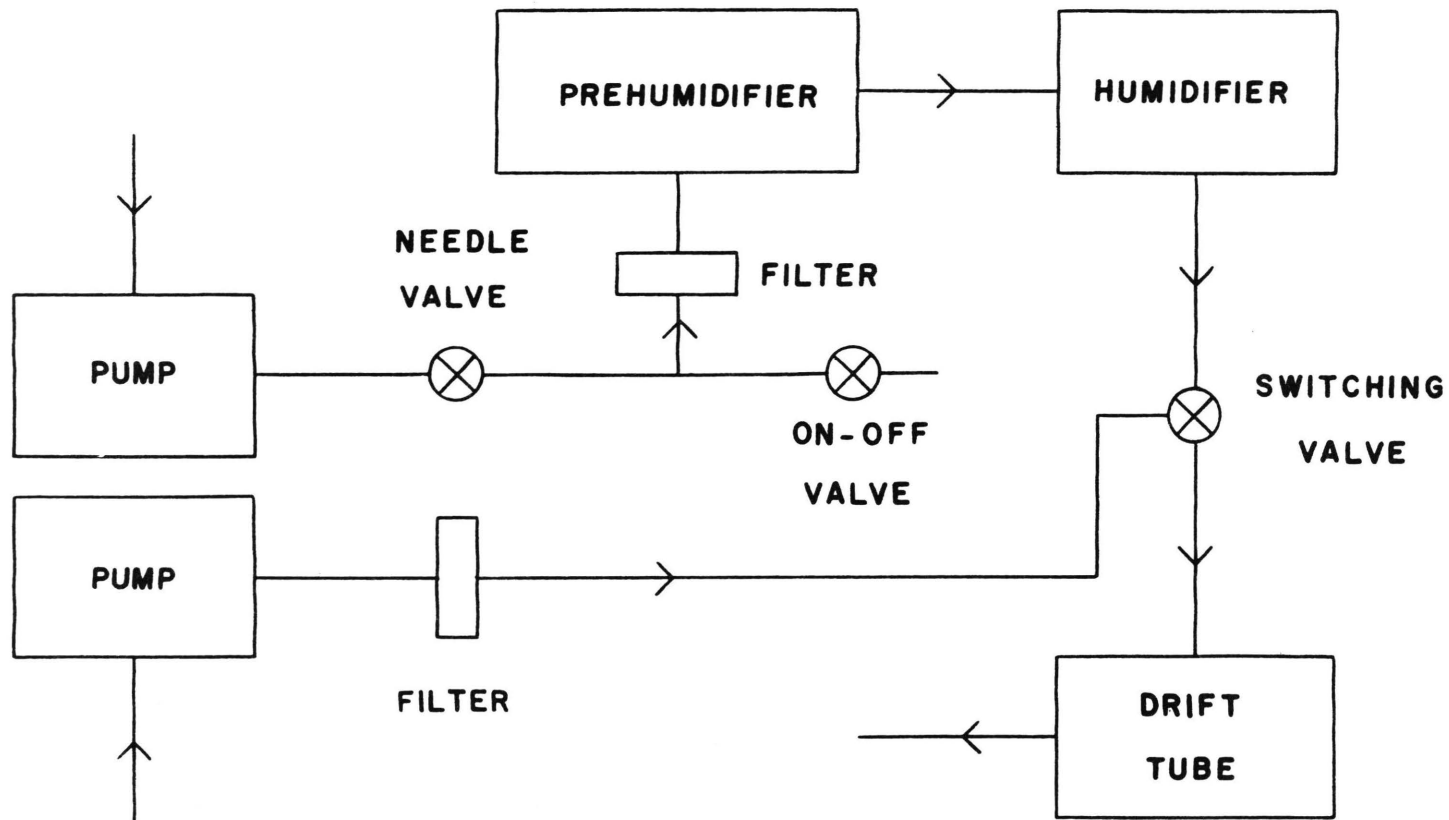


Fig. 2. Overall block diagram of humidification system

#### D. Water Baths and Temperature Sensors

Two stirred, constant temperature, water baths, thermostated at different temperatures, were used. One was 50 cm x 20 cm x 20 cm and provided constant temperature for the drift tube, while the other was 50 cm x 40 cm x 40 cm and provided constant temperature for the humidifier. The temperature in both baths was maintained constant to  $\pm 0.01^{\circ}\text{C}$  by immersion heaters, controlled with mercury-contact thermostats.

The difference in temperature between the two baths was measured by a pair of copper-constantan thermocouples. The potential difference between these two thermocouples was measured with a Leeds and Northrup K-5 potentiometer with a sensitivity of 0.02 microvolts. This difference, when converted to temperature, is a measure of the under-saturation of the air, or the dew point depression, in the drift tube. The actual temperature of the drift tube bath was obtained by a total immersion mercury thermometer, readable to  $0.05^{\circ}\text{C}$ .

#### E. Nuclei Generating Systems

Three different methods for generating the condensation nuclei used in the cloud chamber were employed in the course of these experiments.

For the data on the evaporation of uncontaminated drops, room air nuclei were used. These were injected into the chamber, usually through a Millipore filter ( $8.0\mu\text{m}$  pore

size), by a rubber squeeze bulb.

For much of the data for dodecanol contaminated drops a heated anodized aluminum trough, containing the SAM, was used (see Fig. 3). The vapors from the heated SAM were pumped through a condensing chamber where they condensed into particles which could act as condensation nuclei. The condensing chamber was a 28 cm long x 9 cm diameter glass tube, half-filled with water. The SAM particles then passed through an absolute filter to reduce the concentration entering the cloud chamber. For additional details on this system an earlier paper (10) will be helpful.

The second nuclei generator (see Fig. 4) used to produce the contaminated drops was an Environmental Research Corporation Model 7300 atomizer-impactor. This instrument used prefiltered compressed air to atomize an SAM-ethanol solution. The air then passed through an impactor where particles greater than  $2\mu\text{m}$  diameter were eliminated. A second portion of the prefiltered air was mixed with the air containing the ethanol solution droplets which remained in order to evaporate the ethanol, leaving what was assumed to be pure SAM nuclei. Finally, these particles passed through a radioactive deionizer to neutralize any charges and exited from the generator. The nuclei then passed through 3/8 in I.D. Tygon tubing to a diluter (see below). Bleed lines and clamps along this tubing allowed the volume flow rate of the nuclei-air stream to be adjusted. After dilution, the nuclei went through the condensing chamber.

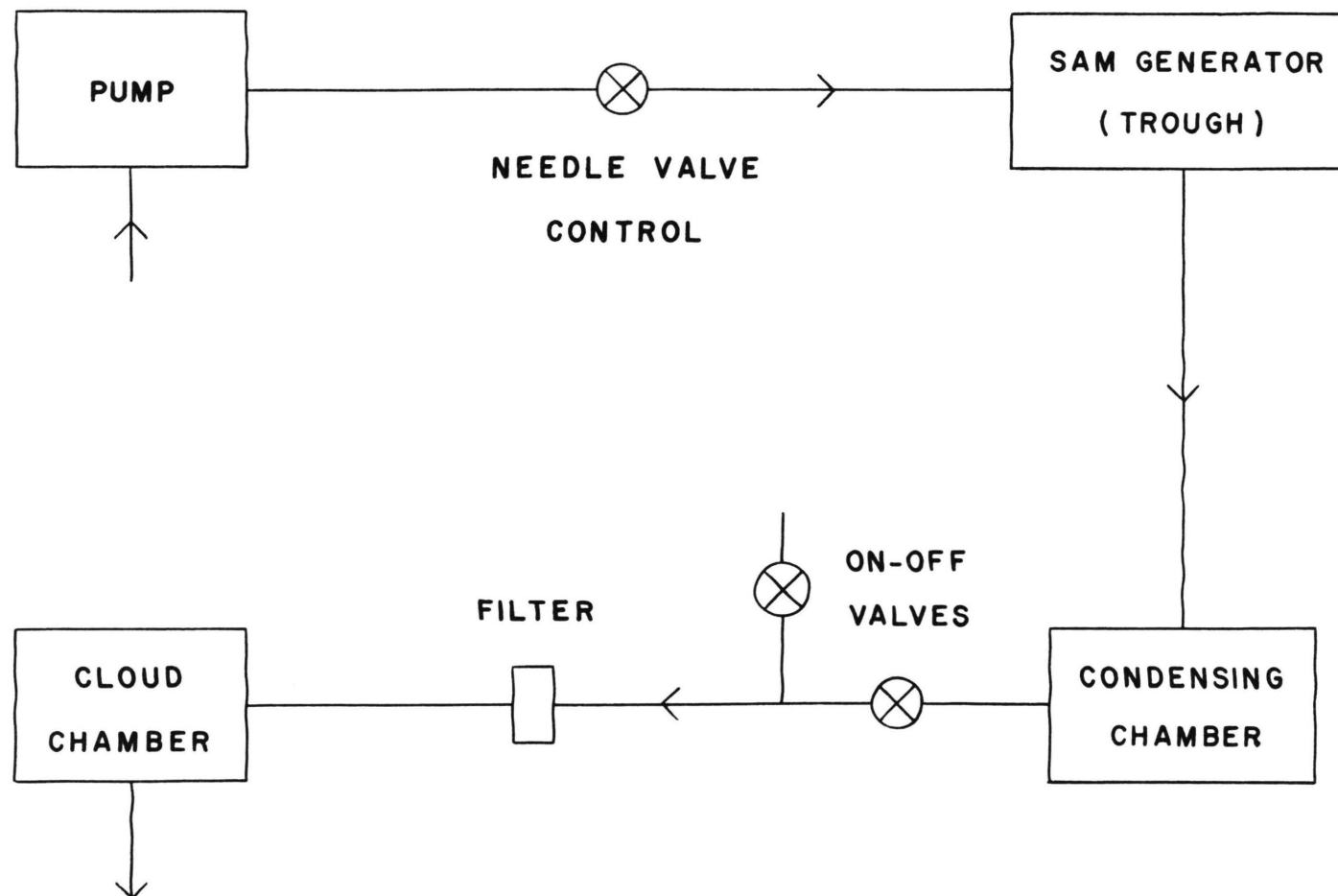


Fig. 3. Nuclei generating system (trough method)

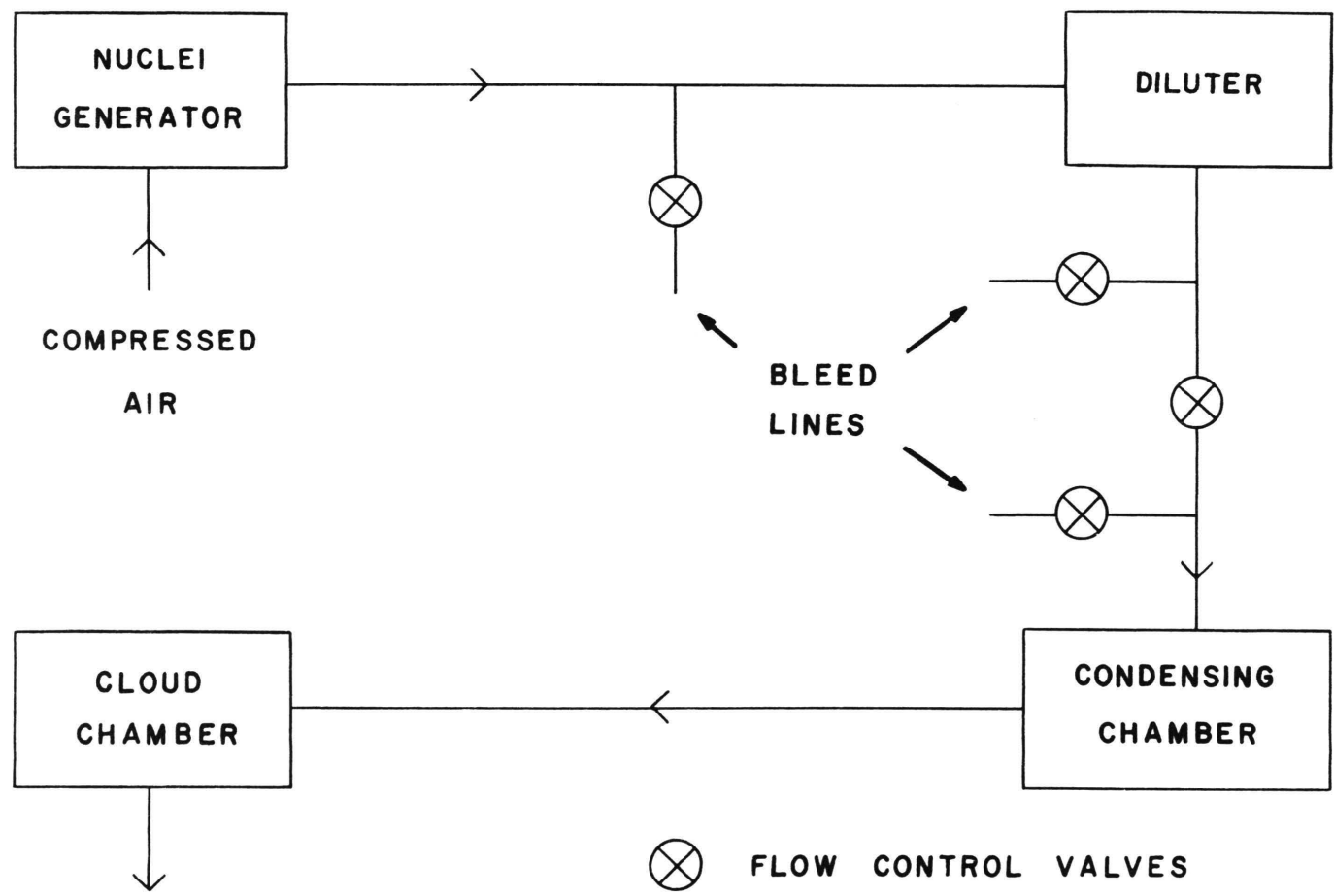


Fig. 4. Nuclei generating system (atomizer-impactor method)

In this case, its sole purpose was to provide humidity for the air stream prior to entry into the cloud chamber. The nuclei-air stream then passed directly to the cloud chamber without filtration.

The diluter was an Environmental Research Corporation Model 740 and consisted of three dilution stages. Each stage consisted of an absolute (HEPA) filter with a bundle of capillary tubes passing through the filter material. It is assumed that all the particles in the air passing through the filter material are removed. This amounts to about 90% of the total air flow. The remaining 10% passed through the capillaries in which it is assumed there is no removal of particles. Thus, the air suffered an approximate 10 to 1 dilution in each stage. Either one, two or three stages could be used, giving a 10, 100 or 1000 to 1 dilution. The diluter was used to provide a usable concentration of nuclei in the cloud chamber. If too many nuclei were present, the drops would either be too numerous or, possibly, too small to be visible when they reached the drift tube. If too few nuclei were available, the drop concentration was so low that an insufficient number reached the drift tube. In our work the diluter was normally set to provide a 100 to 1 dilution ratio.

#### F. Camera System

To photograph the drops as they fell, an Automax Model G-1, 35 mm movie camera, produced by Traid Corporation, was

used. An f/3.5 Micro-Nikkor lens with 55 mm focal length was adapted to the camera. The framing rate was 2.0 frames/sec throughout the experiment.

The camera was mounted on a fixed base about 10 inches from the center of the drift tube and with the optical axis making an angle of about  $30^\circ$  with the incident light used for illumination. This angle provided the greatest scattered intensity from the drops without interference from the incident beam.

The light source used was a 30 cm long, GE 1000-T-31CL quartz bulb. The light was collimated by a cylindrical lens and the width of the beam further reduced by masking the lamp housing so that the emitted beam was 1 cm wide. The center of the beam was alligned with the center of the drift tube and the hole in the bottom plate of the cloud chamber.



#### IV. EXPERIMENTAL PROCEDURE

The majority of the data reported herein was taken at 30.0°C and at dew point depressions from 0.1 to 0.5°C. Thus, the temperature of the drift tube bath was usually maintained at  $30.00 \pm 0.05^\circ\text{C}$ . The humidifier bath was adjusted to a temperature equal to 30.00°C minus the dew point depression. The permissible range of dew point depressions was determined by practical considerations. At depressions less than 0.1°C, condensation of water on the walls of the drift tube made photographing the drops impossible. At depressions much greater than 0.5°C, the drops evaporated too rapidly.

With the baths at constant temperature the run sequence was started (refer to Fig. 2). Filtered room air was first pumped through the drift tube for at least 45 minutes in order to dry the walls and tubing of any residual moisture which may have collected since the last run. Next, the valve was turned to connect the drift tube to the humidifier system. The second pump was then turned on and room air was pumped through the prehumidifier, humidifier and drift tube at a rate of 2 liters per minute. This was continued for 40 minutes to insure that the air in the drift tube would be at the proper humidity. At the end of this time the following were accomplished in rapid sequence. First, the reservoir in the top plate of the cloud chamber was filled with hot water. If surface-active nuclei were to be used, the

compressed air to the nuclei generator was turned on. Then some of the water was forced out of the reservoir onto the bottom of the sintered plate to insure that there was sufficient water in the cloud chamber to form drops. During this latter time a hole in the chamber wall was opened to avoid forcing water or excess humidity into the drift tube. The nuclei were then injected, about 5 seconds for SAM nuclei or 3 squeezes of the rubber bulb for room air nuclei. The pump was turned off, the valve between the drift tube and the humidifier closed and the sliding door in the bottom of the cloud chamber was opened to allow the drops to fall into the drift tube. When a drop concentration corresponding to no greater than 5 drops per film frame was achieved, the camera was started. Concentrations greater than this caused difficulty in following individual drops when the film was read and produced the possibility for interaction between drops. If more than a minute elapsed before the drop concentration was favorable, the run was discontinued in case the humidity in the drift tube might have changed. No more than 70 photographs were taken during one run, since this was the maximum that could be easily handled in the developing process. Immediately following the run, the potential difference between the thermocouples in the drift tube and humidifier baths was read. This difference corresponded to the dew point depression for that run. After this, drying of the drift tube was again begun and the cycle repeated. If the SAM nuclei generator had been used,

the solution reservoir, atomizer and impactor were cleaned before the next run.

## V. RESULTS

Table 1 shows a typical example of data obtained for a dodecanol-contaminated drop at  $\Delta T_{DP} = 0.275^\circ\text{C}$  and with a magnification factor of 5.8 (see below). The method of obtaining the evaporation rate,  $-d(a^2)/dt$ , from data such as that listed in Table 1, was identical for all the drops. A microfilm reader was used to observe the photographs of the falling drops and the magnification factor mentioned above was the ratio of the apparent distance on the microfilm reader to the actual distance inside the drift tube. This magnification factor was obtained by photographing a grid of wires with known average separations and comparing the apparent distance between the wires on the microfilm reader to the known separation. In Table 1,  $\Delta S_{app}$  is the apparent change in position of a falling drop in 0.5 second, as read from the microfilm reader on two successive film frames. The actual velocity,  $v$ , is the average velocity of the droplet between the two exposures and is given by

$$v = \frac{\Delta S_{app}}{(MF) \times 0.5 \text{ sec}} \quad (13)$$

where MF = magnification factor. This value was assumed to be the true velocity at a time midway between the two exposures.

Maxwell's theory, eq. 2, predicts that the rate of change of  $a^2$  with time,  $-d(a^2)/dt$ , should be constant at a

Table 1. Data obtained for an evaporating droplet with magnification factor = 5.8

<u>Film frame number</u>	<u><math>\Delta S_{app}</math> (mm)</u>	<u>v (mm/sec)</u>	<u><math>a^2</math> (<math>\mu m^2</math>)</u>	<u>Average elapsed time (sec)</u>
1	17.3	5.96	51.1	0.25
2	15.7	5.41	46.4	0.75
3	14.5	5.00	42.8	1.25
4	13.3	4.41	37.8	1.75
5	11.8	4.07	34.9	2.25
6	10.9	3.76	32.2	2.75
7	10.4	3.59	30.8	3.25
8	8.9	3.09	26.5	3.75
9	8.0	2.78	23.8	4.25
10				

given dew point depression. To relate the velocity,  $v$ , to the size of the drop, Stokes' Law was used

$$v = a^2/K_s \quad (14)$$

where  $K_s = 9\eta/2(\rho_l - \rho_a)g$ . The values of the constants used to determine  $K_s$  are listed in Table 2. Then, the data for each drop,  $a^2$  vs.  $t$ , were fitted with a straight line;

$$a^2 = a_o^2 - \gamma t \quad (15)$$

The slope of this line,  $\gamma$ , is considered to be the evaporation rate of that drop.

The rates,  $\gamma$ , obtained by the above method were then plotted against the dew point depression,  $\Delta T_{DP}$ . Equation 2 predicts that these data should also yield a straight line. In a previous paper (8) it was shown that the evaporation rate of drops, formed on room air nuclei in the same apparatus as used in the present investigation, agreed most closely with the simple diffusion theory of Maxwell, as opposed to such theories as Kinzer and Gunn (35) and Fuchs (6). While the data presented in a paper by Hughes and Stampfer (10) and in this work have altered the linear coefficients slightly, the best correspondence is still with the Maxwell theory. For this reason, the data for the uncontaminated drops and for the SAM contaminated drops which show a linear relation are treated in the same way

Table 2. Physical constants

<u>Property</u>	<u>Value at temperature</u>		<u>Units</u>	<u>Reference</u>
	<u>30°C</u>	<u>35°C</u>		
Viscosity of air	185.6	188.0	μ poise	(36)
Density of air	1.101	1.077	gm/liter	(37)
Thermal conductivity of air	$6.148 \times 10^{-5}$	$6.229 \times 10^{-5}$	$\frac{\text{cal}}{\text{sec-cm-}^\circ\text{K}}$	(38)
Density of water	0.996	0.994	gm/cm <sup>3</sup>	(37)
$K_s = \frac{9\eta}{2(\rho_l - \rho_a)g}$	8.569	8.694	$\frac{\text{micron}^2\text{-sec}}{\text{mm}}$	Calculated from Stokes' Law
Diffusion coefficient	0.270	0.278	cm <sup>2</sup> /sec	(39)
Coefficient of T from $\rho_{\text{equil}} = bT + c$	$1.60 \times 10^{-6}$	$2.03 \times 10^{-6}$	$\frac{\text{gm}}{\text{cm}^3\text{-}^\circ\text{K}}$	(37)
Heat of vaporization of water	579.5	576.8	cal/gm	(36)

as in Duguid and Stampfer (8), i.e.

$$-\frac{d(a^2)}{dt} = \beta_{\text{exp}} \Delta T_{\text{DP}} + R_0 \quad (16)$$

where  $\beta_{\text{exp}}$  is the experimentally determined slope and  $R_0$  is the y-intercept which would be zero if true agreement with Maxwell were observed.

For the evaporation rate of uncontaminated drops, three sets of data are available, the results of which are shown in Table 3. In Fig. 5 only the data for the uncontaminated drops at 30.0°C, which have been obtained in this work are depicted. The lines in this figure are those obtained from the combined data of Duguid (8) and Hughes (10) and in this work. We will use the data for all three sets of uncontaminated drops at 30.0°C as a baseline for comparison to the SAM-contaminated water drops.

The data for the drops grown on SAM nuclei were processed in a similar fashion and are shown in Fig. 6 to 12. While the data for many of the compounds studied could be described by a linear equation, those of other substances, ethyl myristate, ethyl caprate and decanoic acid, seemed best fit with a quadratic expression. For each compound for which a range of dew point depressions has been studied, both a linear and quadratic expression were determined. The curve most appropriate to the data is shown in the figure for each compound and the coefficients for these expressions are listed in Tables 4 and 5. The dashed line in these



Table 3. Comparison of data for uncontaminated drops at 30°C

<u>Data</u>	<u>Number of drops</u>	<u><math>\beta_{\text{exp}}^*</math></u>	<u><math>R_o^*</math></u>
Duguid	182	$19.1 \pm 0.8$	$0.2 \pm 0.2$
Hughes	117	$19.6 \pm 1.6$	$0.1 \pm 0.4$
Duguid and Hughes (combined)	299	$19.3 \pm 0.7$	$0.1 \pm 0.2$
This work	85	$18.6 \pm 1.6$	$0.3 \pm 0.5$
All data	384	$19.2 \pm 0.6$	$0.1 \pm 0.1$

\*Error limits at 95% confidence level

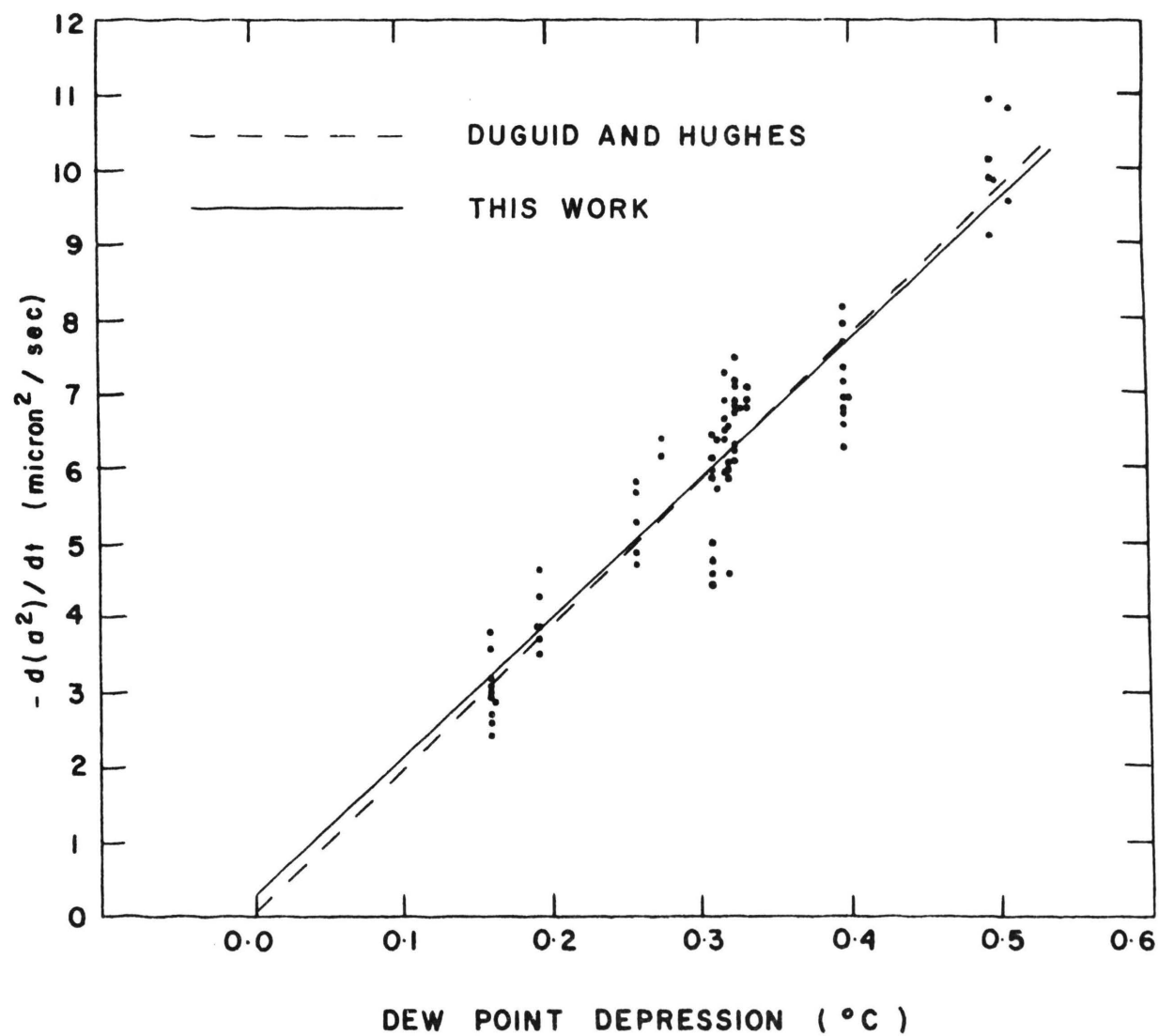


Fig. 5. Evaporation rates of uncontaminated water drops at 30°C

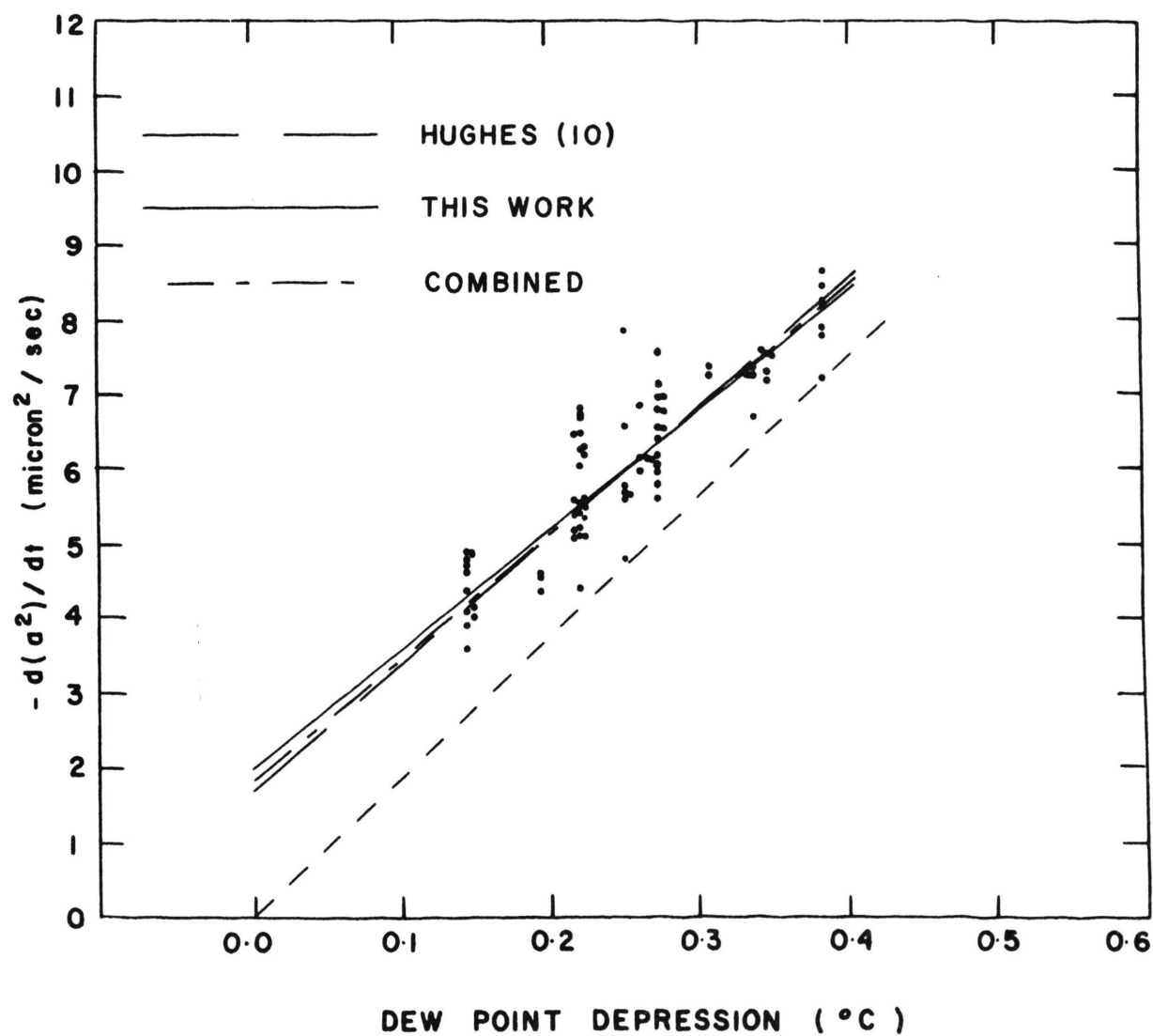


Fig. 6. Evaporation rates of dodecanol contaminated water drops at  $30^{\circ}\text{C}$

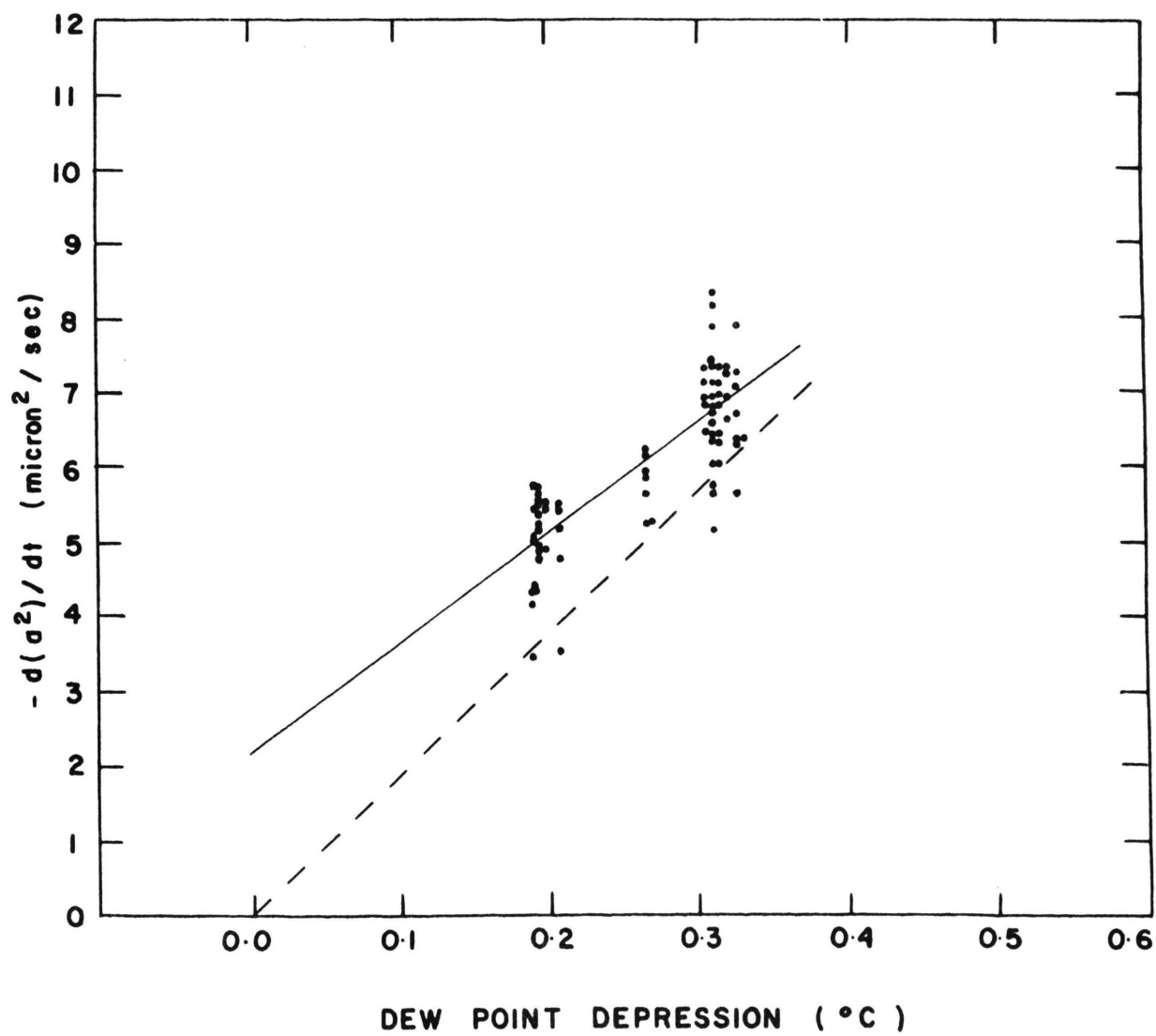


Fig. 7. Evaporation rates of Igepal CO-430 contaminated water drops at 30°C

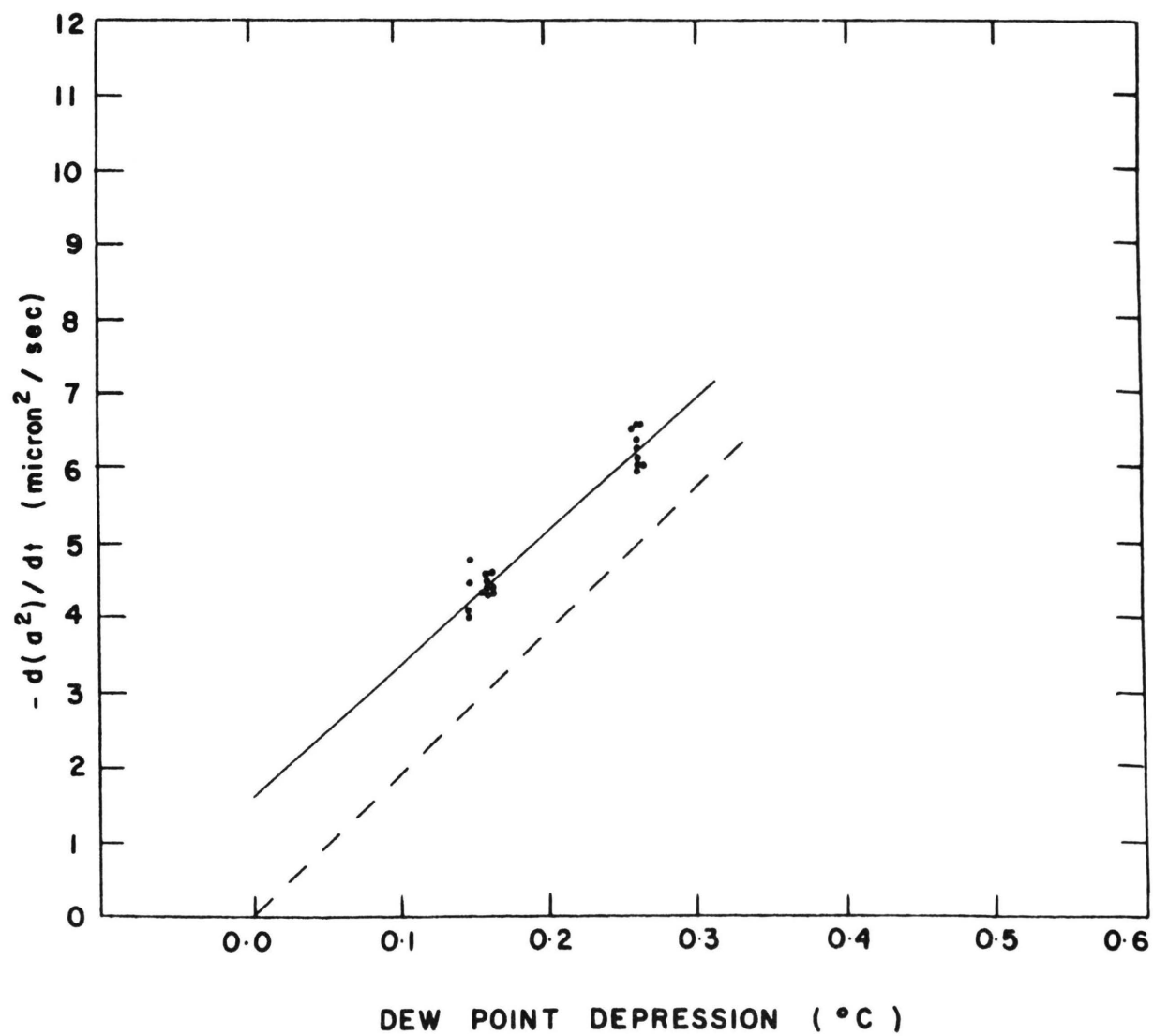


Fig. 8. Evaporation rates of Igepal CO-730 contaminated water drops at 30°C

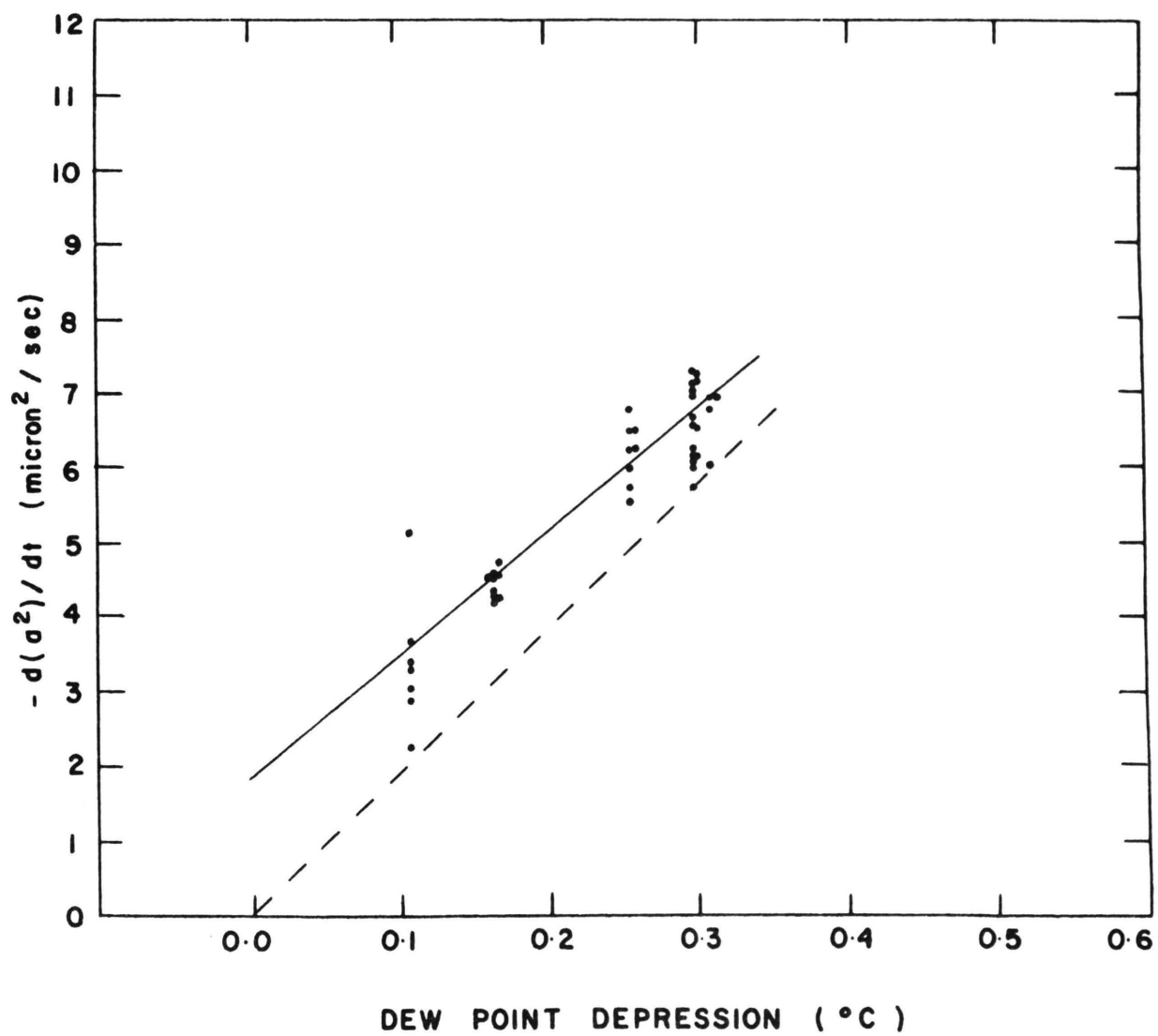


Fig. 9. Evaporation rates of hexadecane contaminated water drops at 30°C

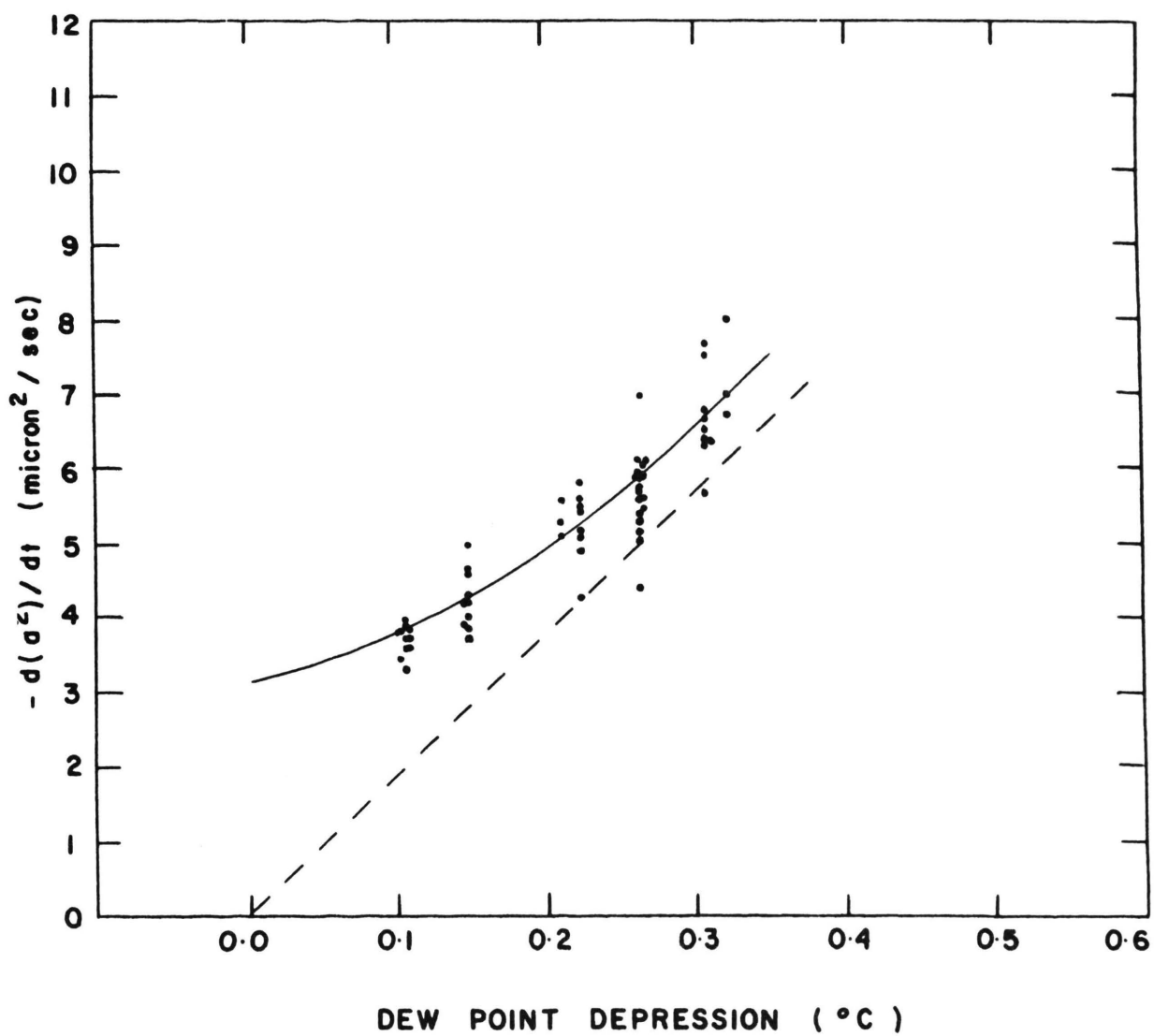


Fig. 10. Evaporation rates of decanoic acid contaminated water drops at  $30^{\circ}\text{C}$

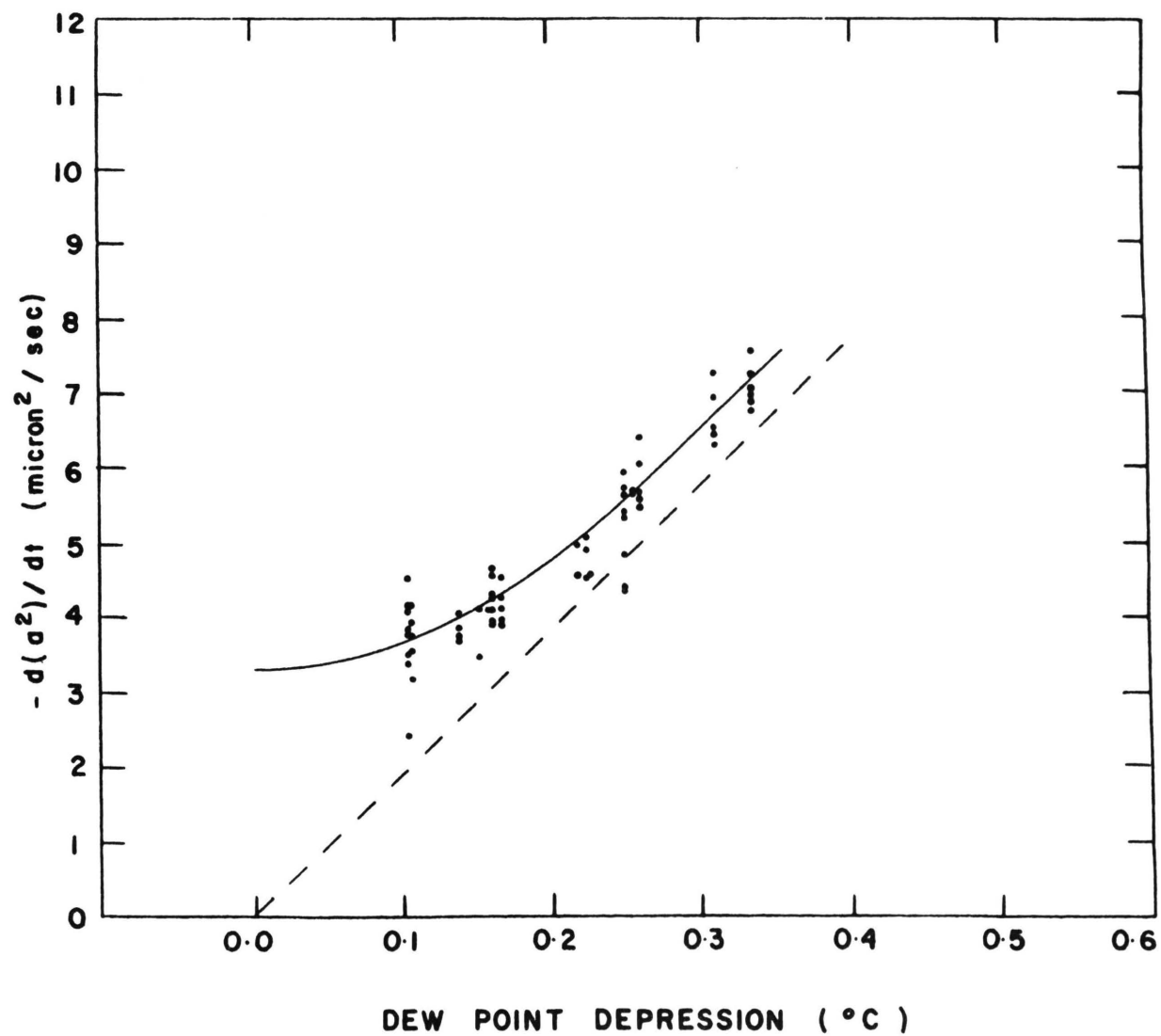


Fig. 11. Evaporation rates of ethyl myristate contaminated water drops at 30°C



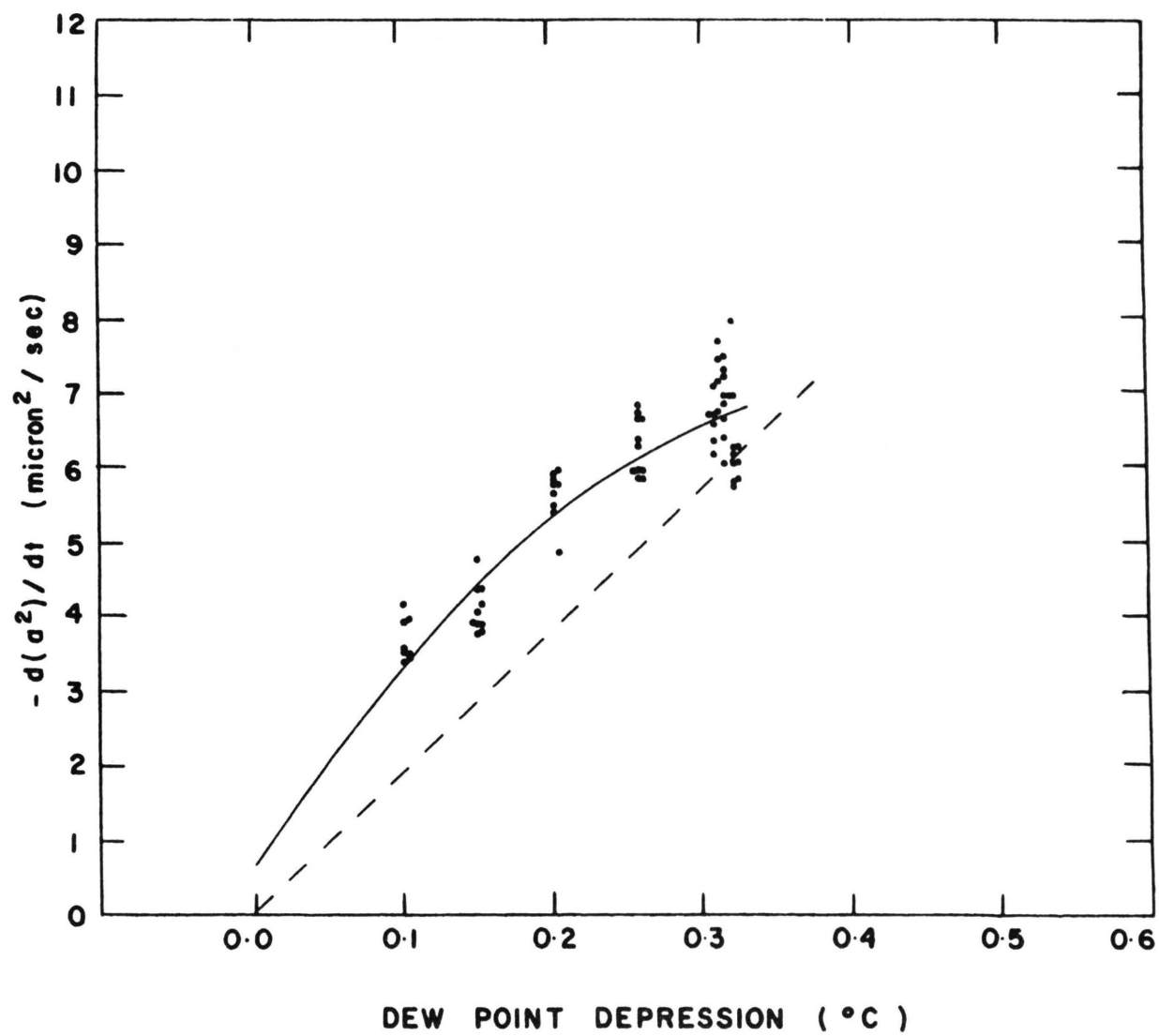


Fig. 12. Evaporation rates of ethyl caprate contaminated water drops at 30°C

Table 4. Linear\* least squares coefficients\*\*

<u>Compound</u>	<u><math>\beta_{\text{exp}}</math></u>	<u><math>R_o</math></u>	<u>Number of drops observed</u>
Pure	18.6 $\pm$ 1.6	0.3 $\pm$ 0.5	85
Dodecanol	16.0 $\pm$ 1.4	2.0 $\pm$ 0.4	103
Igepal CO-430	15.2 $\pm$ 1.9	2.1 $\pm$ 0.5	85
Igepal CO-730	17.5 $\pm$ 1.8	1.6 $\pm$ 0.4	21
Hexadecane	16.2 $\pm$ 1.8	1.8 $\pm$ 0.4	49
Decanoic acid	13.9 $\pm$ 1.7	2.1 $\pm$ 0.4	63
Ethyl myristate	14.5 $\pm$ 1.4	2.0 $\pm$ 0.3	68
Ethyl caprate	13.7 $\pm$ 1.6	2.4 $\pm$ 0.4	71

\*  $-d(a^2)/dt = \beta_{\text{exp}}(\Delta T_{\text{DP}}) + R_o$

\*\* Error limits at 95% confidence level

Table 5. Quadratic\* least squares coefficients\*\*

<u>Compound</u>	<u><math>\gamma_Q</math></u>	<u><math>\beta_Q</math></u>	<u><math>\alpha_Q</math></u>	<u>Number of drops observed</u>
Pure	-4.0 $\pm$ 12.6	21.2 $\pm$ 8.2	-0.1 $\pm$ 0.5	85
Dodecanol	-12.2 $\pm$ 15.0	21.9 $\pm$ 7.8	1.4 $\pm$ 0.4	103
Igepal CO-430	3.3 $\pm$ 28.3	13.7 $\pm$ 12.8	2.2 $\pm$ 0.5	85
Igepal CO-730	41.6 $\pm$ 4.3	—	3.3 $\pm$ 0.4	21
Hexadecane	-27.9 $\pm$ 40.5	27.9 $\pm$ 17.0	0.8 $\pm$ 0.4	49
Decanoic acid	29.8 $\pm$ 27.5	1.6 $\pm$ 11.4	3.2 $\pm$ 0.4	63
Ethyl myristate	35.1 $\pm$ 18.1	-0.5 $\pm$ 7.8	3.4 $\pm$ 0.3	68
Ethyl caprate	-40.9 $\pm$ 26.5	31.9 $\pm$ 11.9	0.6 $\pm$ 0.4	71

$$* - d(a^2)/dt = \gamma_Q (\Delta T_{DP})^2 + \beta_Q (\Delta T_{DP}) + \alpha_Q$$

\*\* Error limits at 95% confidence level

figures shows the evaporation rate of uncontaminated drops.

In the case of dodecanol (Fig. 6), an earlier set of data (10) is available. In Table 6 a comparison of those data with the results found in this investigation is presented and these three sets of results are plotted in the figure.

Table 6. Comparison of data for dodecanol contaminated drops at 30°C

<u>Data</u>	<u>Number of drops</u>	<u><math>\beta_{exp}^*</math></u>	<u><math>R_o^*</math></u>
Hughes (10)	120	$17.5 \pm 1.5$	$1.7 \pm 0.4$
This work	103	$16.0 \pm 1.4$	$2.0 \pm 0.4$
Combined	223	$17.0 \pm 1.0$	$1.8 \pm 0.3$

\*Error limits at 95% confidence level

The points shown, however, are only those obtained in this investigation. In all other figures, the data from this work are the only available information. Table 7 lists the data for compounds which were studied at a single dew point depression. (The pure drop rate at  $\Delta T_{DP} = 0.31^\circ\text{C}$  is 6.06.)

Table 7. Results of compounds studied at a single dew point depression

<u>Compound</u>	<u>Number of drops</u>	<u><math>\Delta T_{DP}</math> (<math>^\circ\text{C}</math>)</u>	<u>Evaporation rate (<math>\mu\text{m}^2/\text{sec}</math>)</u>
5-decanol	11	0.31	7.15
1-chlorohexadecane	5	0.31	7.45

Table 8 lists results of an experiment in which the drift tube bath temperature,  $T_2$ , was 35.0°C, instead of the usual 30.0°C.

Table 8. Enhanced evaporation rates at  $T_2 = 35.0^\circ\text{C}$

<u>Compound</u>	<u>Number of drops</u>	<u><math>\Delta T_{DP}</math> (<math>^\circ\text{C}</math>)</u>	<u>Evaporation rate (<math>\mu\text{m}^2/\text{sec}</math>)</u>
Pure	10	0.22	5.02
Pure (Duguid (8))	-	0.22	5.08
Dodecanol	7	0.21	5.72
Igepal CO-430	6	0.22	6.13

## VI. EXPERIMENTAL ERROR

One possible error in the experimental technique would be an imprecise knowledge of the magnification factor. An error in the magnification factor could cause a difference in the measured evaporation rate for all the drops from their true value at that dew point depression. However, this could only result in a systematic error and would not explain the widely varying measured rates for different drops in a single run. To prevent errors caused by the magnification factor, the calibration grid (see Results section) was photographed periodically, so that at any time an error in the evaporation rate due to this factor was less than 2%.

In obtaining the drop position on the film frame, three procedures could introduce errors: positioning of the film in the reader, marking the location of the drop, and measuring the distance between drop positions in two successive film frames. The easiest way to evaluate these errors was their collective effects on the evaporation rate. The same three drops on one run were read on five different days. The rates obtained for the individual drops were  $6.36 \pm 0.35$ ,  $6.14 \pm 0.21$  and  $6.06 \pm 0.44$ . This yields a maximum error of 15% in obtaining the rate of a single drop and is the only error source found to date capable of producing the scatter observed in the data at a single dew point depression. As an important value in determining whether drops on any single

run are consistent with past data is their average evaporation rate, an additional evaluation was done with the following results. The average rate of the three drops was  $6.18 \pm 0.06$ , giving a maximum error in this value of 2.1%. All confidence limits were calculated at the 95% level.

The framing rate of the camera was checked in two ways. First, periodically, the length of time required to take 60 photographs was determined. This led to a possible error of 0.8% between successive frames. A second and more accurate method was used on one occasion. A timer, readable to 1/60 second, was photographed by the camera for 20 seconds. It was determined that the time between successive frames was constant and within 0.4% of the 0.5 second value assumed for the framing rate in the experiment.

The last error source in measuring was the determination of the dew point depression. Duguid (8) has previously quoted an error of  $\pm 0.01^\circ\text{C}$  and no disagreement in this value was justified by the measurements in this work.

In order to evaluate the effect of the SAM surface coverage as a possible source of the variation of evaporation rates at a single dew point depression, a plot of  $-d(a^2)/dt$  vs. the median value of the radius was made. The plot exhibited only random scatter, indicating no coverage effects, if the nuclei are assumed to be monodisperse. A second test involved a least squares quadratic fit of the  $a^2$  vs.  $t$  data for the dodecanol and ethyl myristate contaminated drops to determine if the best fit could be described

as concave upward or downward. A fit which was concave upward would indicate that the evaporation rate of that drop was greater in the first half of its observed lifetime. The reverse is true for a concave downward fit. However, the data showed approximately equal numbers of concave upward and downward curves, again indicating no effects of surface coverage.

Contamination of the drops was considered carefully. To insure that the drops observed were contaminated by the desired materials, only runs for which uncontaminated drops had been determined to possess the correct evaporation rate before and after that run were used. This eliminated the possibility of contaminants in the cloud chamber and drift tube. A sample of pure ethanol was used periodically in the aerosol generator to insure that nuclei were not being produced from the solvent. Usually, a few drops were produced but in a concentration that would be far too sparse for use in a normal run.

As noted above, the rate determined in this work, using the atomizer-impactor method of nuclei generation, gave results comparable to those of Hughes (10) using a heated trough. However, as a further check that the measured rates were not dependent upon the method of generation of the SAM nuclei, data were obtained with dodecanol and hexadecane using the trough method (see Apparatus section). Both compounds yielded results consistent with past data using the atomizer-impactor method and, thus, the two generating



systems were considered equivalent.

The largest source of possible contamination was the ethanol used as a solvent to generate the SAM nuclei. However, as reported in the literature (39), at 30°C ethanol enhances the structuring or hydrogen bonding of water. Therefore, even if some of the ethanol solvent, used in the SAM generator, was still present in the drops, the effect should be the opposite of whatever caused the observed increase in evaporation rates.

Other possible sources of error have already been discussed by Duguid and Stampfer (8). These included the slip factor correction, possibilities for a change in humidity inside the drift tube during a run and the existence of convection currents within the drift tube. It was shown that these errors were either insignificant or that there was no evidence for their existence. Nothing was found in this work to change those conclusions.

It should be noted that the data for some of these compounds, particularly dodecanol, were collected over a 2 year period and showed no change in that time. Thus, there is no reason to suspect any unknown changes in either the operating conditions or apparatus. Also, where applicable, the data were consistent with those of Duguid (8) and Hughes (10) so that operating techniques do not appear to be a factor.

Finally, as mentioned by Duguid (8), the supposedly pure or uncontaminated drops were generated on room air

nuclei and are thus not completely pure. Since one of our original contentions was that SAM exists in the atmosphere, it would be surprising if the room air nuclei were SAM-free or that the drops did not contain some of this material. Since differences in the evaporation rates of the pure and SAM-contaminated drops are evident, it would appear that the SAM are either not present in sufficient amounts on a single nuclei or are of a completely different structural type than those involved in this study. This is indicated by the fact that  $R_0$  (see eq. 16) for the pure drops has a value of about 0.1, while for the SAM-contaminated drops  $R_0$  ranges from 1.6 to 2.4. Therefore, the increases in evaporation rates found in this study and in that of Hughes (10) are probably minimal and the true increase, compared to pure water, is actually greater.

## VII. DISCUSSION OF RESULTS AND CONCLUSIONS

From the data presented above it appears that the principal cause of the observed increase in evaporation rates, due to the SAM used in this study, was the presence of an alkyl chain. In addition, it is possible, although not entirely obvious, that there may be an effect of the hydrophilic groups of the SAM, which adds to (in the case of 1-chlorohexadecane) or subtracts from (in the cases of ethyl myristate, ethyl caprate and decanoic acid) the enhanced evaporation due to the hydrophobic alkyl chain. The following discussion is designed to illuminate aspects of this enhanced evaporation.

At the beginning of this work it was thought that this enhanced evaporation was a function of the hydrophilic group as well as the chain length of the alkyl group. If this were true, different classes of compounds should cause different evaporation rates at the same dew point depression. However, as can be seen from the graphs, there is little difference in the evaporation rates of drops when SAM with primary or secondary hydroxyl or ethylene oxide polar groups are present. Even an aliphatic hydrocarbon with no polar group present, exhibits almost identical effects. That such small differences should exist between these compounds is surprising. The lack of any effect of the length of the alkyl chain has already been observed by Hughes and Stampfer (10) for dodecanol and hexadecanol. The absence of

differences caused by SAM with primary versus secondary hydrophilic groups, the lack of effect on the rate by hydrophobic chain length or even the absence of any polar group point to the fact that the evaporation rate enhancement is mainly due to the presence of a long hydrocarbon chain. This would be the conclusion drawn from examining the data of dodecanol, 5-decanol, hexadecane and the Igepal compounds. However, data for other compounds, especially ethyl myristate and decanoic acid, appear slightly different and introduce the possibility that the hydrophilic groups also may have some importance.

From Figs. 10 and 11 it can be seen that decanoic acid and ethyl myristate contaminated water drops appear to evaporate with a rate equal to or possibly greater than the dodecanol contaminated drops at low  $\Delta T_{DP}$ , but as  $\Delta T_{DP}$  increases their rates fall below those exhibited in the case of dodecanol. Since the hydrophilic group in both these compounds is the same ( $-\text{CO}_2-$ ), it was expected that ethyl caprate would exhibit a similar effect. In fact, the data for this latter compound show a lower rate at only the highest dew point depression studied,  $0.32^\circ\text{C}$  (see Fig. 12), which makes the quadratic expression fitted to the data appear different. However, it was felt that these compounds, because of their similar structure should be treated together.

Finally, it should be noted that the drops contaminated with 1-chlorohexadecane appear to evaporate slightly faster

than hexadecane.

In the manner in which the data have been treated and presented above, it has been assumed that the rate of evaporation of an individual drop is constant, i.e.  $-d(a^2)/dt = \text{constant}$ , eq. 1. However, assuming no loss of SAM, the fraction of the surface area which is covered by SAM continually increases as the drop evaporates. Thus, it would be logical to expect that the rate of evaporation would change with time and the temporal change of the total surface area would be better described with a curve rather than a straight line. To check this possibility, a quadratic expression was fit to the data for the 180 drops contaminated by dodecanol and ethyl myristate. One would expect that if the rate of evaporation is a function of surface coverage, the coefficient of the squared term in the quadratic would be non-zero. Further, the curvature should be more pronounced the greater the fractional decrease of the radius. In Table 9 are listed the frequencies of occurrence of the sign of this term (a negative sign implies that the rate increases with the surface coverage) for various fractional decreases of the radius. The coefficient was considered zero if its absolute value was less than 0.1. As can be seen, there appears to be no predominant pattern in the signs of the coefficients. This indicates that there was no appreciable effect of the surface coverage on the evaporation rate.

Unfortunately, we have no absolute measure or

Table 9. Frequency of occurrence of the sign of  $\gamma_Q$  as a function of the percentage change of the radius

Dodecanol contaminated drops

	$\frac{a_{\text{initial}} - a_{\text{final}}}{a_{\text{initial}}} (\times 100)$										
	<u>0-3</u>	<u>3-6</u>	<u>6-9</u>	<u>9-12</u>	<u>12-15</u>	<u>15-18</u>	<u>18-21</u>	<u>21-24</u>	<u>24-27</u>	<u>&gt;27</u>	<u>Total</u>
$\gamma_Q < 0$	0	0	5	4	8	6	4	9	4	3	43
$\gamma_Q = 0$	0	1	2	0	0	1	3	4	2	2	15
$\gamma_Q > 0$	0	4	4	2	3	12	10	5	2	3	45

Ethyl myristate contaminated drops

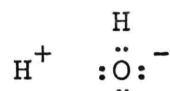
$\gamma_Q < 0$	0	7	1	6	7	4	2	1	0	0	28
$\gamma_Q = 0$	0	1	0	1	5	2	0	1	0	3	13
$\gamma_Q > 0$	0	3	5	5	4	3	2	2	1	1	26

calculation of the extent of the surface coverage. It is assumed that at no time are the drops completely covered, because, if such were the case, there would undoubtedly be a marked decrease in the evaporation rate (41) when this occurred. This assumption allows a calculation of the maximum size of the SAM nuclei on which the water drops were formed. This size is approximately  $0.4\mu\text{m}$  radius. An attempt was made to determine the size of the nuclei directly with a Climet Model 201 particle counter and Nuclear Data Model 2200 pulse height analyzer. Because of the difficulty of calibrating the particle analyzer in this size range with liquid particles and the low signal to noise ratio in the measurements, the sizes could only be estimated. The best median value appeared to be about  $0.2\mu\text{m}$  radius. Finally, the size of the nuclei could be calculated from the concentration of SAM in the ethanol solution used in the generator. Assuming the cut-off radius of the impactor used was  $1\mu\text{m}$ , the calculated radius of the SAM residues was  $0.2\mu\text{m}$ . In summary then, a reasonable estimate of the surface coverage is a minimum of 5%, when a drop first comes into the field of view of the camera, and 25% at the end of the time it is followed, with a maximum possible coverage at any time of 100%.

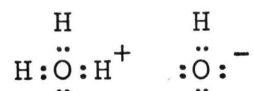
At the outset of any explanation of a phenomenon observed in aqueous solutions, the difficult and controversial subject of water structure must be approached. Many differing theories (42-45) for the structure of pure water

exist and they seem to come into favor or disrepute as each new paper is published. Because of this situation one must choose a model on the basis of how well it agrees with the observed phenomenon. Following this line of thought, we will use the flickering-cluster model of water structure as proposed by Frank and Wen (42) and developed by Nemethy and Scheraga (43,46,47). Although other models of water structure may be just as well founded, this model seemed to provide the easiest interpretation of the observed increase in the evaporation rates.

Frank and Wen theorized that a resonance structure could be written for the water molecule as shown below



This molecule could then interact with a neighbor because of this partial charge separation and form a hydrogen bond.



These molecules, in turn, can form hydrogen bonds with their neighbors. This cooperative effect leads to the formation of clusters of hydrogen bonded water molecules. These "flickering clusters" are continually being created and destroyed due to local energy fluctuations in the liquid. They must not be viewed as rigid crystalline structures, but



as flexible entities continuously forming and disappearing in different regions of the bulk water. Nemethy and Scheraga also state that there is a limit to the size of the clusters and the model predicts that at 30°C the median cluster consists of seven water molecules.

Nemethy and Scheraga (46) have used this model to describe the modification of water structure near hydrocarbon solutes. Water near nonpolar solutes, including hydrocarbon chains, has been determined (42,48) to possess enhanced structure or hydrogen bonding. Nemethy and Scheraga (46) state that this is caused by a shift in the energy states due to the presence of a nonpolar solute. The different energy states cause an increase in the relative number of fully-bonded water molecules, i.e. four-bonded, and a decrease in the number of water molecules possessing one, two three or no hydrogen bonds near the solute molecule. In the paper by Frank and Wen (42) it is stated that the non-polar solute, because of its feeble electrostatic interactions, acts as a shield from disruptive influences on one boundary of the cluster, thus prolonging the clusters' average lifetime. Whatever the true explanation, nonpolar solutes act to enhance structure in these models. However, this enhanced structuring is probably not continuous around large molecules. Just as there are limits to the sizes of clusters in pure water, the clusters near the nonpolar solutes can grow only so large, so that two or more clusters would probably exist along large hydrocarbon

chains. Between the clusters, unbonded water molecules can still exist. The conclusion drawn from this model is that long alkyl chains should enhance water structure. Since this implies that the water molecules are held more tightly in the liquid, it would be expected that the rate would be lower than that found for pure drops. This means that since an increased, and not decreased, evaporation rate has been observed, there must be another factor, not considered by the model.

Davies, Ormondroyd and Symons (33) have studied aqueous solutions of tetraalkyl ammonium salts by nuclear magnetic resonance. They found that, in the presence of these salts, the NMR peak due to hydrogen bonded water moved from negative to positive values (using pure water as a reference equal to zero) as the temperature changed from 273°K to 353°K. A negative value of the NMR shift indicates that there is more order or hydrogen bonding present than in pure water at that temperature; a positive value indicates less hydrogen bonding. Although the tetraalkyl ammonium salts are ionic solutes, the regions near the alkyl chains of these salts are considered to show effects similar to nonpolar solutes. Thus, these salts do show the enhanced structuring observed in other works (32,34,42) and predicted by the Nemethy and Scheraga model. However, this effect disappeared at higher temperatures. Davies, Ormondroyd and Symons also observed that for symmetrical tetraalkyl ammonium salts the transition from negative to positive NMR

shifts occurred at progressively lower temperatures as the alkyl chain length increased from ethyl (343°K) to butyl (303°K). Since there appeared to be a chain length effect, the octyl trimethyl ammonium salt was also examined. The NMR shift for this ion became positive at about 275°K. They concluded that long alkyl chains overcome their normal structure enhancing properties because of increased thermal agitation of the chain. This agitation ruptures or weakens hydrogen bonds, producing less order than in pure water. Even though the work of Davies, Ormondroyd and Symons was concerned with bulk solution effects, the same properties should exist at the surface, although possibly modified.

This seems to provide an explanation for the increased evaporation rates observed in our experiments. However, as an introductory note, let us first consider the evaporation process for a drop at temperature  $T_1$ . For a water molecule to have a chance of evaporating, it must be in the surface and exist as a monomer, not as part of a cluster. Next, it must possess sufficient energy to escape the surface and enter the vapor phase immediately adjacent to the drop surface. Here, along with other water molecules which have escaped the surface, it contributes to the term  $\rho_s$ , eq. 1. To evaporate the water vapor molecules must be able to diffuse away from the vicinity of the drop. The best reason to assume a diffusion controlled process for evaporation is an experiment by Archer and La Mer (49). They found that a small number of holes (about 1% of the surface area) in a

monolayer caused the monolayer to lose its usual evaporation retardation ability and the normal rate of evaporation of pure water was observed. This means that the number of monomers available at the liquid surface is not rate determining. Monomers still had time to fill the vapor space adjacent to the drop surface and attain  $\rho_s$ . Therefore, diffusion of water vapor away from the drop is the rate controlling step and the evaporation is vapor diffusion controlled. The driving force for this process is the vapor concentration gradient,  $\rho_s - \rho_\infty$ . Now, if the temperature of the drop is raised to  $T_2$ , an average water molecule will possess more energy and thus will have a greater chance of entering the vapor phase adjacent to the drop. This, by increasing  $\rho_s$ , will increase the diffusional driving force and elevate the evaporation rate. To return now to the ideas of Davies, Ormondroyd and Symons, the thermally induced vibrations of the alkyl chain would tend to cause the hydrogen bonded clusters to be ruptured and impart extra energy to the water molecules. Thus, the addition of SAM to a water drop seems to provide the same effect on the evaporation rate as an increase in temperature for a pure water droplet.

As noted earlier, drops contaminated with ethyl myristate, ethyl caprate and decanoic acid have shown lower rates than those with hexadecane for certain values of  $\Delta T_{DP}$ . NMR shift studies (50,51,52) have shown that many polar groups, carboxyl and carboxylic esters included, act as

structure makers, i.e. increase the amount of hydrogen bonding in the region adjacent to them over that which would be found in bulk water. This increased hydrogen bonding could be the explanation for the lower rates, as compared to a compound such as dodecanol, caused by these three compounds in the high dew point depression regions (see Figs. 10, 11 and 12). However, why, at low  $\Delta T_{DP}$ , there appears to be little difference remains unexplained. Conversely, the chloride ion has been reported to have a structure breaking effect. Therefore, 1-chlorohexadecane would be expected to enhance the evaporation rate of the water drops as much or more than hexadecane. As can be seen from Table 7, this was the case. 1-chlorohexadecane treated drops exhibited an average rate of 7.45 at  $\Delta T_{DP} = 0.31^{\circ}\text{C}$ , while the hexadecane treated drops produced a rate of 6.80. While this evidence is by no means conclusive, it does lend support to the hypothesis that there is some polar group effect.

Drost-Hansen (27) has proposed that at  $30^{\circ}\text{C}$ , a change between two forms of ordered water structures can occur near SAM. During this process of structural conversion, an increase in the number of monomers could occur and thus possibly increase the evaporation rates in the presence of SAM. If this is the explanation for the increased evaporation rates, then at higher or lower temperatures, where it is proposed there is only one enhanced structure, the evaporation rate should not be increased. However, as Table 8 shows, the increased rate is observed at  $35^{\circ}\text{C}$  also.

Although this does not disprove the idea that some change takes place at 30°C, it does indicate that there must, at the least, be other phenomena which are also important.

In an earlier paper by Hughes and Stampfer (10), it was suggested that the increased evaporation could be a result of "spurting", the ejection of tiny jets of water from the surface (Kingdon (26), Berg and George (53)). Within our present hypothesis there is still room for such a phenomenon, but it is no longer necessary.

## REFERENCES

1. Altshuller, A. P., Reactivity of organic substances in atmospheric photooxidation reactions. U. S. Department of Health, Education, and Welfare. Public Health Service Publication 999-AP-14, July 1965.
2. Robinson, E., and Robbins, R. C., Sources, abundance and fate of gaseous atmospheric pollutants. Stanford Research Institute, Project PR-6755 (1968).
3. Blanchard, D. C., Sea-to-air transport of surface active material. Science 146, 396 (1964).
4. Barger, W. R., and Garrett, W. D., Surface active organic material in the marine atmosphere. J. Geophys. Res. 75, 4561 (1970).
5. Munson, E., and Hughes, W. J., unpublished data.
6. Fuchs, N. A., "Evaporation and Droplet Growth in Gaseous Media." Pergamon Press, New York, 1959.
7. Fuchs, N. A., Concerning the velocity of evaporation of small droplets. Phys. Z. Sowj. 6, 224 (1934); NACA Tech. Memo. 1160, August 1947.
8. Duguid, H. A., and Stampfer, J. F., Jr., The evaporation rates of small, freely falling water drops. J. Atmos. Sci. 28, 1233 (1971).
9. Duguid, H. A., A study of the evaporation rates of small freely falling water droplets. M.S. Thesis, University of Missouri-Rolla, 1969.
10. Hughes, R. B., and Stampfer, J. F., Jr., Enhanced evaporation of small, freely falling water drops due to surface contamination. J. Atmos. Sci. 28, 1244 (1971).
11. Deryaguin, B. V., Fedoseyev, J. F., and Rosenzweig, L. A., Investigation of the adsorption of cetyl alcohol vapor and the effect of this phenomenon on the evaporation of water drops. J. Colloid Interface Sci. 22, 45 (1966).
12. Snead, C. C., and Zung, J. T., The effects of insoluble films upon the evaporation kinetics of liquid droplets. J. Colloid Interface Sci. 27, 25 (1968).

13. Eisner, H. S., Quince, B. W., and Slack, C., The stabilization of water mists by insoluble monolayers. Disc. Faraday Soc. 30, 86 (1960).
14. Kocmond, W. C., Garrett, W. D., and Mack, E. J., Modification of laboratory fog with organic surface films. J. Geophys. Res. 77, 3221 (1972).
15. Garrett, W. D., Retardation of water drop evaporation with monomolecular surface films. J. Atmos. Sci. 28, 816 (1971).
16. La Mer, V. K., and Barnes, G. T., The effects of spreading technique and purity of sample on the evaporation resistance of monolayers. Proc. Natl. Acad. Sci. U.S. 45, 1274 (1959).
17. Tovbin, M. V., and Savinova, E. V., The kinetics of nonsteady state processes at the liquid-gas interface. Zhur. Fiz. Kim. 21, 2717 (1957).
18. James, L. K., Jr., and Berry, D. J. O., Evaporation enhancement by protein films. Science 140, 312 (1963).
19. Sebba, F., and Rideal, E. K., Permeability in monolayers. Trans. Faraday Soc. 37, 273 (1941).
20. Bull, H. B., Studies on surface denaturation of egg albumin. J. Bio. Chem. 123, 17 (1938).
21. Derjaguin, B. V., Bakanov, S. P., and Kurghin, I. S., The influence of a foreign film on evaporation of liquid drops. Disc. Faraday Soc. 30, 96 (1960).
22. Zung, J. T., Meeting of the American Chemical Society, Symposium on Evaporation Rate Analysis, New York, 1969.
23. O'Grady, V. J., The maximum rate of vaporization of water with dissolved salts and surface contamination. Ph.D. Thesis, University of Pennsylvania, 1971.
24. Beredjick, N., Treatment to accelerate evaporation of distillate and retard evaporation of condensate. U.S. Patent 3,220,934, 1965.
25. Leonov, L. F., and Prokhorov, P. S., Influence of surface-active substances on the evaporation of fine water drops. Izvestiya Akademii Nauk. SSSR, Seriya Khimicheskaya 4, 735 (1967).



26. Kingdon, K. H., Enhancement of the evaporation of water by foreign molecules adsorbed on the surface. J. Phys. Chem. 67, 2732 (1963).
27. Drost-Hansen, W., Molecular aspects of aqueous interfacial structures. J. Geophys. Res. 77, 5132 (1972).
28. Horne, R. A., ed., "Water and Aqueous Solutions: Structure, Thermodynamics and Transport Processes." Wiley (Interscience), New York, 1972.
29. Horne, R. A., "Marine Chemistry." Wiley (Interscience), New York, 1969.
30. Franks, F., in "Hydrogen-Bonded Solvent Systems" (A. K. Covington and P. Jones, eds.). Taylor and Francis Ltd., London, 1968.
31. Horne, R. A., "Marine Chemistry", p. 48. Wiley (Interscience), New York, 1969.
32. Jolicoeur, C., The, N. D., and Cabana, A., Near infrared spectra of water in aqueous solutions of organic salts. Can. J. Chem. 49, 2008 (1971).
33. Davies, J., Ormondroyd, S., and Symons, M. C. R., Proton nuclear magnetic resonance shifts for water containing alkylammonium ions. Chem. Comm., 1204 (1971).
34. Wen, W., in "Water and Aqueous Solutions: Structure, Thermodynamics and Transport Processes", Chap. 15 (R. A. Horne, ed.). Wiley (Interscience), New York, 1972.
35. Gunn, R., and Kinzer, G. D., The terminal velocity of fall for water droplets in stagnant air. J. Meteor. 6, 243 (1949).
36. "International Critical Tables of Numerical Data, Physics, Chemistry and Technology." McGraw-Hill, New York, 1926.
37. "Handbook of Chemistry and Physics" (Charles D. Hodgman, ed.), 44th edition. Chem. Rubber Publ. Co., Cleveland, 1963.

38. Taylor, W. J., and Johnston, H. L., Thermal conductivity measurement. J. Chem. Phys. 14, 219 (1946).
39. Reid, R. C., and Sherwood, T. K., "The Properties of Gases and Liquids." McGraw-Hill, New York, 1958.
40. Clifford, J., and Pethica, B. A., Properties of micellar solutions, Part 2. Trans. Faraday Soc. 60, 1483 (1964).
41. LaMer, V. K., ed., "Retardation of Evaporation by Monolayers: Transport Processes." Academic Press, New York, 1962.
42. Frank, H. S., and Wen, W., III. Ion-solvent interaction Structural aspects of ion-solvent interaction in aqueous solutions: A suggested picture of water structure. Disc. Faraday Soc. 24, 133 (1957).
43. Nemethy, G., and Scheraga, H. A., Structure of water and hydrophobic bonding in proteins. I. A model for the thermodynamic properties of liquid water. J. Chem. Phys. 36, 3382 (1962).
44. Bernal, J. D., and Fowler, R. H., A theory of water and ionic solution, with particular reference to hydrogen and hydroxyl ions. J. Chem. Phys. 1, 515 (1933).
45. Hagler, A. T., Scheraga, H. A., and Nemethy, G., Structure of liquid water. Statistical thermodynamic theory. J. Phys. Chem. 76, 3229 (1972).
46. Nemethy, G., and Scheraga, H. A., Structure of water and hydrophobic bonding in proteins. II. Model fro the thermodynamic properties of aqueous solutions of hydrocarbons. J. Chem. Phys. 36, 3401 (1962).
47. Nemethy, G., and Scheraga, H. A., The structure of water and hydrophobic bonding in proteins III. The thermodynamic properties of hydrophobic bonds in proteins. J. Phys. Chem. 66, 1773 (1962).

48. Frank, H. S., and Evans, M. W., Free volume and entropy in condensed systems III. Entropy in binary liquid mixtures; Partial molal entropy in dilute solutions; Structure and thermodynamics in aqueous electrolytes. J. Chem. Phys. 13, 507 (1945).
49. Archer, R. J., and La Mer, V. K., The rate of evaporation of water through fatty acid monolayers. J. Phys. Chem. 59, 200 (1955).
50. Butler, R. N., and Symons, M. C. R., Solvation spectra Part 29 - Nuclear magnetic resonance studies of electrolyte solutions: Ion-solvent interactions in methanol. Trans. Faraday Soc. 65, 2559 (1969).
51. Davies, J., Ormondroyd, S., and Symons, M. C. R., Solvation spectra Part 41 - Absolute proton magnetic resonance shifts for water protons induced by cations and anions in aqueous solutions. Trans. Faraday Soc. 67, 3465 (1971).
52. Davies, J., Ormondroyd, S., and Symons, M. C. R., Solvation spectra Part 42 - Influence of quaternary ammonium and carboxylate ions on the proton magnetic resonance spectrum of water. Trans. Faraday Soc. 68, 686 (1972).
53. Owe Berg, T. G., Trainor, R. J., Jr., and Vaughan, U., Stable, unstable and metastable charged droplets. J. Atmos. Sci. 27, 1173 (1970).

## VITA

David Alan Sierawski was born on August 1, 1948 to Francis and Lola Sierawski in St. Louis, Missouri. He attended St. Louis Preparatory Seminary South, where he received his diploma in May, 1966. His college education was obtained from the University of Missouri-Rolla. He received a B.S. in Chemistry from the University of Missouri-Rolla in May, 1971. During the period from September, 1968 to January, 1971 he was associated as a co-op with the Inorganic Research Division of Monsanto Company. On August 11, 1972 he was married to Patricia Ann Russo. He has been enrolled, as a candidate for a Masters Degree in Chemistry, at the University of Missouri-Rolla since June, 1971 and has had a National Science Foundation research assistantship during that time.

## APPENDIX

## LIST OF SYMBOLS

$a$	radius of drop
$a_0$	initial radius of drop
$b, c$	coefficients in equation, $p_{\text{equil}} = bT + c$
$g$	gravitational acceleration
$\ell$	thickness of the boundary diffusion layer
$m$	mass of drop
$m_1$	mass of a liquid molecule
$m_2$	mass of a vapor molecule
$r$	evaporation rate, $-dm/dt (1/4\pi a^2)$ , at time $t$
$r_0$	stationary evaporation rate, $-dm/dt (1/4\pi a^2)$ , at $t = 0$
$t$	time
$v$	velocity
$\bar{v}$	mean velocity of gas molecules at the given temperature
$C_0$	vapor concentration in the surrounding medium corresponding to $C_p$
$C_p$	equilibrium concentration of liquid in a saturated solution of the monolayer material
$C_\infty$	concentration of the surrounding gaseous medium at an infinite distance from the drop surface
$D$	diffusion coefficient of water vapor in the surrounding gaseous medium
$D_1$	diffusion coefficient of liquid molecules through a given monolayer
$I_F$	evaporation rate, $-d(a^2)/dt$ , according to Fuchs
$I_M$	evaporation rate, $-d(a^2)/dt$ , according to Maxwell

$I_Z$	evaporation rate, $-dm/dt$ , according to Zung
$K$	coefficient of thermal conductivity
$K_S$	$9\eta/2(\rho_l - \rho_s)g$
$L$	latent heat of vaporization
$MF$	magnification factor
$\Delta S_{app}$	apparent change in position of a falling drop in 0.5 second, as read from the microfilm reader on two successive film frames
$T_{DP}$	dew point temperature
$T_\infty$	temperature of the surrounding gas at an infinite distance from the drop surface
$\Delta T_{DP}$	dew point depression
$\alpha$	evaporation coefficient
$\alpha_o$	evaporation coefficient for a pure drop
$\alpha_Q, \beta_Q, \gamma_Q$	coefficients of quadratic fit to $-d(a^2)/dt$ vs. $\Delta T_{DP}$ data
$\beta_{exp}, R_o$	coefficients of linear fit to $-d(a^2)/dt$ vs. $\Delta T_{DP}$ data
$\beta_M$	slope of Maxwell line, $-d(a^2)/dt = \beta_M(\Delta T_{DP})$
$\gamma$	slope of line, $a^2 = a_o^2 - \gamma t$
$\delta$	thickness of monolayer
$v$	$(kT/2\pi m_2)^{1/2}$
$\rho_a$	density of air
$\rho_l$	density of liquid
$\rho_s$	density of vapor at the surface of the drop
$\rho_\infty$	density of vapor at an infinite distance from the drop surface
$\Gamma$	$K/DL$
$\Delta$	jump distance